VEGETATION AND CLIMATE INTERACTION PATTERNS IN KYRGYZSTAN: SPATIAL DISCRETIZATION BASED ON TIME SERIES ANALYSIS

Maksim Kulikov and Udo Schickhoff

With 12 figures and 2 tables
Received 16 February 2017 · Accepted 1 June 2017

Summary: Spatio-temporal variations of climate-vegetation interactions in Central Asia have been given a lot of attention recently. However some serious methodological drawbacks of previous studies prevented thorough assessment of such interactions. In order to avoid the limitations and improve the analysis we used spatially explicit time series of NDVI (normalized difference vegetation index), temperature and precipitation which were decomposed to seasonal and trend components on per-pixel basis using STL (seasonal decomposition of time series by loess). Trend and seasonal components of NDVI, precipitation and temperature were assessed pixelwise for temporal correlations with different lags to understand the patterns of their interaction in Kyrgyzstan and adjoining regions. Based on these results a coefficient of determination was calculated to understand the extent to which NDVI is conditioned by precipitation and temperature variations. The images with the lags of time series correlation minima and maxima for each pixel and coefficients of NDVI determination by temperature and precipitation were subjected to cluster analysis to identify interaction patterns over the study area. The approach used in this research differs from previous regional studies by implementation of seasonal decomposition and analyzing the full data without spatial or seasonal averaging within predetermined limits prior to the analysis. NDVI response to temperature and precipitation was assumed to be spatially variable in its sign, strength and lag, thus a separate model was developed for each pixel. The results were assessed with cluster analysis to identify spatial patterns of temporal interactions, decrease dimensionality and facilitate their comprehensiveness. The research resulted in 5 spatial clusters with different patterns of NDVI interaction with temperature and precipitation on intra- and interannual scales. The highest correlation scores between NDVI and temperature at the seasonal scale were found at 0-4 months lag and between NDVI and precipitation at 1-5 months lag. At high elevations of 3000-4000 m above sea level, both precipitation and temperature occurred to be facilitating factors for vegetation development, whereas temperature was rather a limiting factor at lower elevations of 200-1300 m a.s.l. We developed maps of the NDVI coefficient of determination by both temperature and precipitation. Only deserts and glaciers had low coefficients of determination (adjusted R2) on the seasonal scale (0.1-0.3), whereas areas with vegetation were greatly conditioned by temperature and precipitation (0.7-0.95). On the trend scale, dense vegetation and bare areas had low coefficient of determination (0.1-0.3), whereas areas with average vegetation cover were greatly controlled by the climatic factors (0.7-0.9).

Zusammenfassung: Raumzeitliche Veränderungen von Klima-Vegetation-Interaktionen in Zentralasien stehen seit geraumer Zeit im Fokus wissenschaftlichen Interesses. Gewisse Unzulänglichkeiten methodischer Herangehensweisen früherer Studien verhinderten bislang eine gründliche Abschätzung solcher Interaktionen. Um methodische Limitierungen zu vermeiden und entsprechende Analysen zu optimieren, liegen dieser Studie räumlich explizite Zeitreihen von NDVI (normalisierter differenzierter Vegetationsindex), Temperatur und Niederschlag zugrunde, die mittels STL (saisonale Auflösung von Zeitreihen mit Loess) in saisonale und Trend-Komponenten auf Pixelbasis aufgelöst wurden. Die entsprechenden Komponenten von NDVI, Temperatur und Niederschlag wurden pixelweise im Hinblick auf zeitliche Korrelationen unter Berücksichtigung unterschiedlicher Latenzzeiten analysiert, um die Interaktionsmuster von Klima und Vegetation in Kirgistan und angrenzenden Regionen nachvollziehen zu können. Auf der Grundlage der Ergebnisse wurde ein Bestimmtheitsmaß ermittelt, das zur Abschätzung der Abhängigkeit des NDVI von Niederschlag und Temperatur verwendet wurde. Die graphischen Darstellungen mit den Latenzzeiten der Korrelationsmaxima und -minima der Zeitreihen für jedes Pixel und die Bestimmtheitsmaße zur NDVI-Beeinflussung durch Temperatur und Niederschlag wurden Clusteranalysen unterzogen, um die Interaktionsmuster im gesamten Arbeitsgebiet zu identifizieren. Der methodische Ansatz dieser Studie weicht von früheren Regionalstudien insofern ab, als dass die Zeitreihenanalyse mit saisonaler Auflösung umgesetzt und der gesamte Datensatz ohne vorhergehende räumliche oder saisonale Mittelwertbildung analysiert wurde. Die NDVI-Reaktion auf Temperatur und Niederschlag wurde im Hinblick auf Signal, Stärke und Verzögerungszeit als räumlich variabel angenommen, und somit ein separates Modell für jedes Pixel entwickelt. Die Ergebnisse wurden mit Clusteranalysen untersucht, um räumliche Muster und zeitliche Interaktionen zu erkennen, die Dimensionalität zu reduzieren, und deren Vollständigkeit zu optimieren. Als Ergebnis lassen sich 5 räumliche Cluster differenzieren mit unterschiedlichen Mustern der NDVI-Interaktion mit Temperatur und Niederschlag auf intra- und interannueller Ebene. Die höchsten Korrelationen zwischen NDVI und Temperatur auf saisonaler Ebene wurden bei einer Verzögerungszeit von 0-4 Monaten und zwischen NDVI und Niederschlag bei 1-5 Monaten ermittelt. In Höhenlagen zwischen 3000 und 4000 m NN erwiesen sich sowohl Niederschlag als auch Temperatur als die Vegetationsentwicklung begünstigende Faktoren, während

in Höhen zwischen 200 und 1300 m NN die Temperatur eher limitierend wirkt. Die entwickelten Kartendarstellungen zeigen die NDVI-Beeinflussung sowohl durch Temperatur als auch durch Niederschlag. Lediglich Wüsten- und Gletscher-Bereiche weisen geringe Bestimmtheitsmaße (korrigiertes R2) auf saisonaler Ebene auf (0,1-0,3), während vegetationsbedeckte Flächen einen sehr deutlichen Zusammenhang mit Temperatur und Niederschlag zeigen (0,7-0,95). Auf der Trendebene sind Bestimmtheitsmaße bei dichter Vegetation und vegetationslosen Flächen gering (0,1-0,3), Flächen mit gewöhnlicher Vegetationsbedeckung zeigen dagegen eine starke Abhängigkeit von den klimatischen Faktoren (0,7-0,9).

Keywords: climatic change, GIS, Kyrgyzstan, remote sensing, vegetation geography, biogeography

1 Introduction

Climate change has become an important issue in recent decades. It has been drawing lots of attention from researchers and many studies have been conducted on climate change scenarios. Among many regions Central Asia was reported to undergo severe climatic changes (Hijioka et al. 2014). Kyrgyzstan is a mountainous country with prominent altitudinal variation in ecosystems. High geodiversity, i.e. a small-scale variety of abiotic habitat conditions, in particular the climatic ones, induce a conspicuous small-scale variety of vegetation types. According to climate scenarios, Kyrgyzstan will face severe annual and seasonal variations of temperature and precipitation (Lioubimtseva and Cole 2006; Hijioka et al. 2014; Huang et al. 2014). Climate change models for Kyrgyzstan indicate future temperature and precipitation increase above the global mean (Christensen et al. 2007; GoKR 2009; Hijioka et al. 2014). Unsustainable use of natural resources aggravated by the effects of climate change may lead to the loss of valuable ecosystems (Kerven et al. 2011; Crewett 2012; Dörre and Borchardt 2012; Borchardt et al. 2013). Thus, considerable impacts of temperature and precipitation changes on vegetation in both spatial and temporal domains are to be expected, the study of which is crucial for land use economy and climate change adaptation planning.

Many numerical studies have been published aiming at assessing the impact of climatic variables on vegetation in Central Asia. Remotely sensed data and their time series have been intensively used for vegetation cover change analysis as well as forecasting based on different regression models (De Jong 1994; Martinez and Gilabert 2009; Verbesselt et al. 2010; de Jong et al. 2011; Eckert et al. 2015). Recently, a few studies have been conducted in the region looking for vegetation change in spatio-temporal domain and its relation to climatic factors (Nezlin et al. 2005; Propastin et al. 2007, 2008a, 2008b; Kariyeva and Van Leeuwen 2011; Kariyeva et al. 2012; Klein et al. 2012; Gessner et al. 2013; Zhou et al. 2015; Yin et al. 2016; Dubovyk et al. 2016). Covering many important patterns of climate and vegetation interactions, especially in mountain areas with diverse terrain and elevation, these studies have their strengths in several aspects, but some disadvantages in others, namely: considering either temperature or precipitation as the main impact factor, spatial averaging of spatially explicit data time-series within predetermined limits, temporal averaging of temporarily explicit data within predetermined limits, not considering temporal lags between climate impact and vegetation response, or considering them at coarse scale, not considering the seasonal and trend components separately, and using analysis that produce abstract components, which are difficult to interpret.

Methods like PCA (principal component analysis) or EOF (empirical orthogonal functions) do not allow for seasonal and trend decomposition, modelling and forecasting. These methods are good in decreasing data dimensionality; however, the results are difficult to interpret as they represent abstract variables which do not necessarily have real equivalents. Quite often temporal or spatial averaging of the data, which are temporarily and spatially explicit, is used within predetermined spans even before the analysis (Kariyeva and Van Leeuwen 2011; Kariyeva et al. 2012; Dubovyk et al. 2016), which leads to loss of data and simplifies the patterns within those limits. Decrease of spatial data resolution by systematic averaging can lead to signal quality improvement, however averaging within vast geographic areas means certainly the loss of valuable data. The very identification of the limits is biased by human aspects (state borders, seasons) which may have no reflection in nature. Another main assumption, which is not always correct, is that climate and vegetation have similar relations within one generalization unit, or that correlation between vegetation and climatic factors have the same sign throughout the study area. For example, Ichii et al. (2002) looked for correlation between NDVI and climate variables globally. They identified positive and negative correlations between the same variables in different areas.

Considering delayed vegetation response to climatic factors was given a lot of attention (Kariyeva and Van Leeuwen 2011; Kariyeva et al. 2012; Gessner et al. 2013; Dubovyk et al. 2016). But doing it on a coarse temporal scale, as in case of seasonal averaging, may lead to failure to identify strong relationships and exact temporal lags (Kariyeva and Van Leeuwen 2011; Kariyeva et al. 2012; Dubovyk et al. 2016), whereas not considering the temporal lags between climate impact and vegetation response may lead to failure to identify any relationship (Zhang et al. 2016a). Several studies use least squares regression for identification of linear trends in NDVI and climatic factors (Zhou et al. 2016; Yin et al. 2016), some of them consider lagged relationships (Nezlin et al. 2005; Propastin et al. 2007; Gessner et al. 2013; Zhang et al. 2016b). Others employ linear regression with time or climatic factors as predictors and spatially averaged NDVI as a response variable (Propastin et al. 2008b; Eckert et al. 2015). Least squares linear regression is not designed for approximation of trends in natural time series, as they are not stationary and have strong seasonal and trend components, and outliers can have considerable impact. Furthermore, it simplifies the interannual and seasonal interactions of climate and vegetation, does not account for trend cyclic behavior, and leads to failure identifying temporal correlations between them. Sometimes the approaches are not flexible in predictors across pixels, and regression models are stuck using a fixed lag of a predictor for the entire area (Kariyeva and Van Leeuwen 2011; Kariyeva and van Leeuwen 2012; Dubovyk et al. 2016). Rarely have authors used the plethora of time series analysis methods for seasonal decomposition and cross-correlation.

The fact that both temperature and precipitation can have a combined impact on vegetation each with its own time lag, which can vary depending on many factors is often left unconsidered. Using the seasonal and trend decomposition of vegetation and climate raster time series on a per-pixel basis and lagged correlation analysis can improve understanding of interactions between the variables. Many studies consider interactions of NDVI either with temperature or precipitation (Propastin et al. 2008a; de Beurs et al. 2009; Gessner et al. 2013). Whereas Cao et al. (2013) used both precipitation and temperature to identify their impact on NDVI and found them to be the main driving factors, but they did not consider correlation with lags. Potter and Brooks (1998) used NDVI and different climate indices as predictors to demonstrate that about 70-80 % of NDVI variations globally could be explained by climate variables only. Propastin et al. (2008b) found that 75 % of NDVI upward trend during growing season in Central Asia is explained by a combination of temperature and precipitation. Qiu et al. (2014) used wavelet transformation for seasonal decomposition, and also discovered NDVI to be conditioned by both temperature and precipitation on seasonal and interannual scales.

The spatio-temporal dimensionality of the imagery time series remains one of the main constraints for a thorough analysis of the existing remotely sensed vegetation and climate data. Many different sophisticated approaches were developed to deal with this issue (Mennis et al. 2005; Mennis 2010; Petitjean et al. 2012; Small 2012; Lai et al. 2016; Qiu et al. 2016; Militino et al. 2017), however, it is obvious that there is no common framework for spatio-temporal studies dealing with climate and vegetation interaction. Quite often spatial or temporal discretization of a study dataset into geographical subareas or seasons is used. This approach addresses data dimensionality and nonstationarity and provides plausible results (Zhao et al. 2011; Mohammat et al. 2013; Zhang et al. 2013; Du et al. 2015; Song et al. 2016). However, averaging of spatially and temporally explicit data within predetermined areas leads to information loss and bias. Spatially explicit analyses are also often limited to temporal averaging or linear regression for identification of trend magnitude and sign. However, vegetation and climate data are non-stationary having seasonal and trend components, which makes the linear least squares method not applicable for its approximation. Considering different seasons separately (Propastin et al. 2008b; Yin et al. 2016) partly solves the issue of non-stationarity, but excludes the intra-annual assessment. Spatial and temporal averaging is often used in one study simultaneously, representing spatio-temporal interactions separately from different perspectives.

The approaches described above solve the issue at the cost of decreasing the resolution in either spatial or temporal domains, which leads to the loss of data and results. The method we use in this study is different from others used in the spatio-temporal domain due to its flexibility, broad applicability and the comprehensiveness of its results. Seasonal decomposition for each pixel and cross correlation with climatic factors does not produce any abstract objects like principal components or orthogonal functions, which are difficult to interpret. At the same time it provides flexibility in using different lags for different predictors on the pixel level and on seasonal and trend scales separately. Considering the draw-

backs of previous research it is necessary to conduct a study, which consequently deals with the detailed shortcomings and provides a reproducible example for better climate change adaptation planning.

We hypothesize that estimating vegetation and climatic seasonal components at each pixel will automatically discriminate vegetation types on the finest scale available, and reveal their intra-annual patterns for the entire country. We further assume that trend components will indicate vegetation trends for the whole study area and spatially explicit climatic factors can be used to explain the interannual variations. We also assume that temperature and precipitation can have either positive or negative impact on vegetation in different regions and at different temporal scales. With cluster analysis of trend and seasonal components we seek to identify different patterns of vegetation and climate interactions and different vegetation formations. The combination of methods we use deals with spatio-temporal dimensionality of data in a straightforward and intuitive way, identifying seasonal and interannual patterns of vegetation, precipitation and temperature in a spatial manner.

2 Study area

2.1 Geographical extent

The study area covered the territory of the Kyrgyz Republic including close parts of China, Kazakhstan, Tajikistan and Uzbekistan, limited by a rectangle between 38°N - 44°N and 68°E - 81°E (Fig. 1). The study encompasses different ecological zones and topographies including deserts, steppes, forestry areas, highland tundras, hills, mountains, rocks, and valleys, as well as different management systems including agricultural lands, forestry, pasture rangelands and nature reserves. The elevations vary from 200 m to 6000 m above sea level, providing a great variation in vegetation and climate conditions.

2.2 Climate

The distribution of annual precipitation is very uneven and varies from 144 mm in some parts of Issyk-Kul region to 1090 mm in the Fergana valley (Adyshev et al. 1987). The midlands and southwestern slopes of the Fergana range receive the highest amount of precipitation in the country – around 1000 mm per year. Highlands on the northern slope of Kyrgyz ridge, Chatkal ridge and Kemin valley as well as the eastern part of Issyk-Kul region also receive a considerable amount of precipitation – about 1000 mm per year. Talas and Chui valleys, as well as the Osh lowland regions receive considerably less precipitation – 300-700 mm annually. Precipitation decreases to about 200-300 mm annually in the Inner Tian-Shan as air masses lose their humidity crossing the ridges. The driest areas are eastern Issyk-Kul, Batken and the Osh highland region, which receive only 150-200 mm annually (Adyshev et al. 1987). In general, annual precipitation amount in Kyrgyzstan is sufficient for crop cultivation and pastoralism, however, most of the precipitation falls in late winter and spring. Summers are very dry, which necessitates the artificial irrigation of agricultural lands. The amount of precipitation in the same region varies greatly interannually. The variations can reach 250 % in eastern Issyk-Kul region, 530 % in SW Kyrgyzstan, 400 % in Inner Tian-Shan and 260 % in the northern part of the country (Adyshev et al. 1987). Precipitation has an altitudinal gradient, its amount increases up to 3500-4000 m above sea level, higher up the increase decelerates.

The hottest months are July and August. In summer, the temperatures across identical elevations are equal across the country, whereas in winter the difference is conditioned by terrain and can reach 15°C. In general, the south-western part of the country is warmer in summer than the northern part; the temperature may reach more than 40°C in valleys. A strong vertical temperature gradient is exemplified by the average monthly temperature in July which differs by more than 20°C from 4°C at 3600 m up to 27°C at 720 m above sea level (Adyshev et al. 1987). In winter, the lowest temperatures are recorded in mountain valleys and depressions.

2.3 Vegetation

Vegetation types are distributed along distinct altitudinal zones, conditioned by vertical gradients of climatic variables. Latitudinal zonation is less obvious, but also evident as exemplified by the difference between zonal (lowland) vegetation mosaics of North and South Kyrgyzstan. In some cases a longitudinal zoning can be observed, which is connected with local features of small-scale air circulation, e.g. seasonal valley winds, which is the case for the Issyk-Kul valley. The inland position of Kyrgyzstan and its proximity to the deserts of Central Asia defines the general aridity of land-

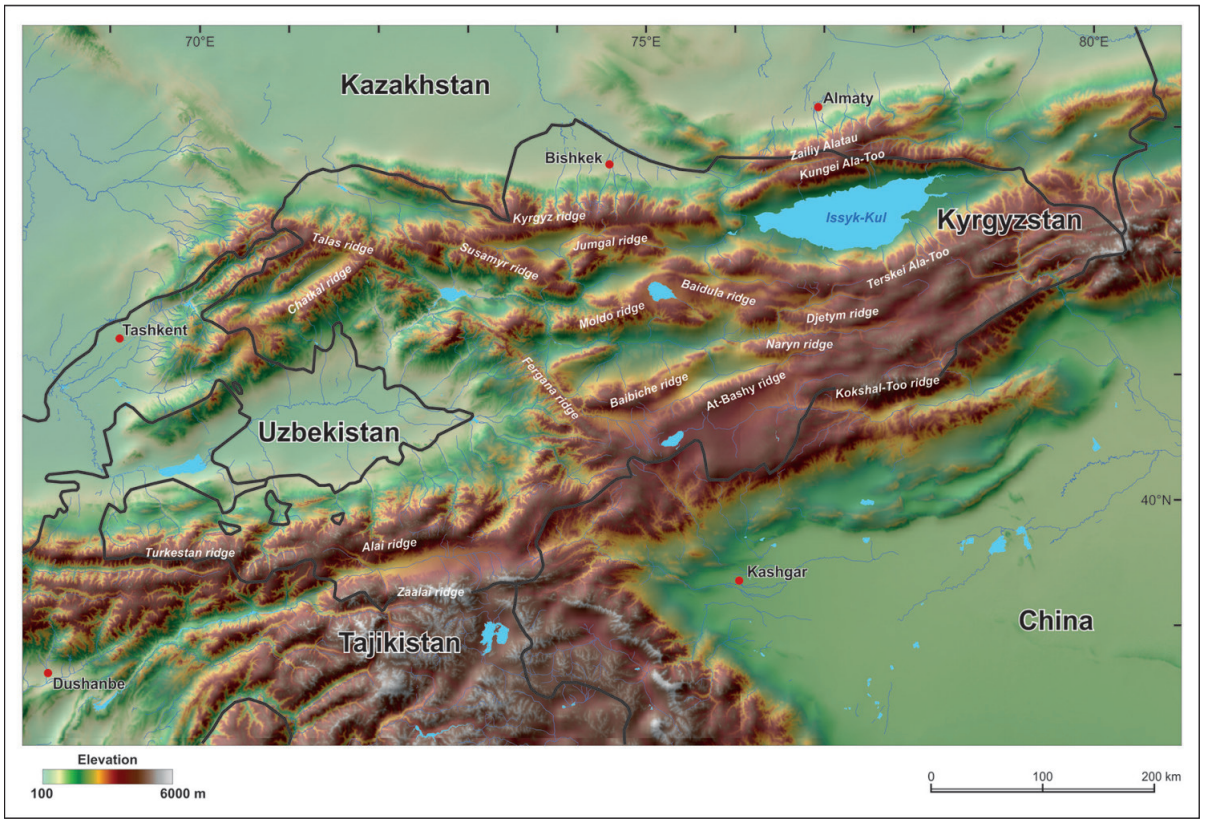

Fig. 1: Study area

scapes and their harsh, exposure-induced contrasts. Arid steppe or desert landscapes occupy about 35 % of the country, while humid landscapes cover only 27 % (ADYSHEV et al. 1987). Due to arid and semi-arid climatic conditions over vast areas, forest and meadow landscapes are often restricted to favorable north-facing slopes.

Midland meadow and steppe landscapes with tall grass on dark soils are prevalent at elevations of 1000-2200 m above sea level. The grassland vegetation interchanges with trees: *Sorbus tianschanica, Juniperus spp., Picea schrenkiana, Acer spp.,* and *Betula spp.* The trees are the remains of forests, the original ecosystem, which was cleared and replaced by grassland vegetation types. Steppes, dominated by *Festuca spp., Stipa spp.,* and *Avena spp.* occupy south-facing slopes interchanged with outcrops of rocks. In the south of the country, *Prangos spp.* are major constituents of these steppe communities (BORCHARDT et al. 2011).

Forests cover only 5.7 % of the country; they are distributed at elevations between 1500-3100 m above sea level. Spruce forests of *Picea schrenkiana* occur in the north and east of the country. Juniper forests occupy almost half of the entire forest area and grow in the south and south-west of the country. The forests are very sparse and dominated by *Juniperus spp., Berberis oblonga*, *Rosa fedtschenkoana*, *Lonicera microphylla*, *Cotoneaster melanocarpus,* and *Spiraea hypericifolia*. The forests on the slopes of Fergana and Chatkal ridges are dominated by *Juglans regia* with other fruit tree species such as *Malus sieversii* and *Malus niedzwetzkyana, Pyrus korshinskyi, Pyrus regelii*, *Prunus sogdiana*, *Ribes janczewskii*, *Prunus mahaleb*, and *Acer turkestanicum*. Riverine forests are developed along river valleys. They are composed of *Populus laurifolia*, *Betula spp.*, *Salix spp.*, *Myricaria elegans*, *Clematis orientalis* and *Hippophae rhamnoides* (ADYSHEV et al. 1987).

Low grass alpine meadows predominate the alpine zone from 3000 m upwards; these are areas of low temperature and a short growing season. The alpine meadows are dominated by *Kobresia spp.*, *Phlomis spp.*, *Geranium spp., Poa alpina*, *Allium semenovii*, *Alchemilla retopilosa*, *Ligularia alpigena*, *Carex spp.*, *Leontopodium spp.*, and *Taraxacum spp.* The meadows interchange with rocky ridges, talus, and snow fields. They mostly occupy valleys and slope bottoms, i.e. the areas where fine particles are deposited and soils have developed.

The upper alpine zone is highland cold desert or tundra, which is distributed at elevations of 3600-3900 m above sea level. Strong insolation results in high evapotranspiration, leaving the soil dry. Highland tundras are very much like zonal tundras, 201 species typical of zonal tundras grow here, including many lichens, mosses, grasses, and sedges. The vegetation is dominated by xerophyte cushion plants, dwarf semishrubs (e.g., *Dryadanthe spp.*), and *Calamagrostis tianschanica* growing in patches. The vegetation cover is very sparse near mountain tops and is dominated by *Smelowskia calycina*, *Richteria spp.,* and *Cerastium lithospermifolium* (Adyshev et al. 1987).

Landscapes of intermontane depressions have arid features. Half-closed depressions such as Chui, Fergana, and Talas valleys have desert-steppe landscapes in their lowest parts giving way to steppes with increasing elevation. These lowland depressions are almost entirely used for irrigated agriculture. The midland depressions of the Inner Tian-Shan have desert-steppe and steppe landscapes. The highland depressions at elevations of 3000-3600 m above sea level are characterized by dry climate, low temperatures and sparse vegetation, which are dominated by *Artemisia spp., Festuca spp.*, and *Ptilagrostis spp.* (Adyshev et al. 1987).

3 Materials

3.1 Data

We used remotely sensed monthly MODIS NDVI, day LST (land surface temperature) and GPCC PRC (precipitation) raster time series of years 2000-2013. MODIS Terra (v5 of MOD13C2 product) monthly NDVI data were used as a general proxy of vegetation conditions, as their relation is well established (Li et al. 2010), and MODIS Terra (v5 of MOD11C3 product) monthly LST (land surface temperature) data for temperature approximation. The quality assessment of the MODIS products did not indicate any serious inaccuracy and missed values. GPCC full data reanalysis version 7.0 (Schneider et al. 2015) monthly precipitation rates with initial spatial resolution of 0.5° were used for approximation of precipitation level.

MODIS land surface temperature and vegetation index data are originally distributed by the Land Processes Distributed Arctive Archive Center (LP DAAC), located at the U.S. Geological Survey (USGS) Earth Resources Observation and Science (EROS) Center (lpdaac.usgs.gov), distributed in netCDF format by the Integrated Climate Data Center (ICDC, http://icdc.zmaw.de) University of Hamburg, Germany. MODIS NDVI is produced regularly every 16 days based on daily recordings, NDVI is derived from atmospherically-corrected reflectance in red and near-infrared spectral bands. MODIS LST is distributed in 0.05° grids, produced by the day/night algorithm from pairs of day and night MODIS observations in seven TIR bands (thermal infrared).

The monthly precipitation data we used were those of GPCC (Global Precipitation Climatology Centre) Full Data Reanalysis Version 7.0 with spatial resolution of 0.5° (Schneider et al. 2015). The data represent a centennial reanalysis of monthly global land-surface precipitation based on the measurements of 75 000 stations world-wide. They contain the monthly totals on a regular grid with a spatial resolution of 0.5°. The temporal coverage of the dataset ranges from January 1901 till December 2013.

We used SRTM (Shuttle Radar Topography Mission) for the digital elevation model. The data were acquired by radar on board of Endeavour shuttle in February 2000, which was a joint project of the National Aeronautics and Space Administration (NASA) and the National Geospatial-Intelligence Agency (NGA). The data resolution is approximately 1 arc-second, which is about 30 m and is provided in 1x1 degree tiles.

The study area was limited by a rectangle between 38°N - 44°N and 68°E - 81°E (Fig. 1). The precipitation, NDVI, LST and SRTM images were all resampled to the same resolution, extent and coordinate system with b-spline resampling. We have chosen the resolution of the MODIS dataset to avoid data loss. As a result, we have got raster images with 184 x 115 pixels, with a pixel size of 5700 m. in WGS84 UTM43N projected coordinate system.

3.2 Tools

Free open source software packages were used for the data analysis. The GIS manipulations and analysis were done in SAGA GIS 2.3.1 (Conrad et al. 2015), time series decomposition and analysis were done in R 3.3.1 (R CORE TEAM 2016), data management and routine automatization were done with Python 3.5 (PYTHON SOFTWARE FOUNDATION 2016). The maps for the publication were prepared with QGIS 2.18.3 (QGIS DEVELOPMENT TEAM 2017).

4 Methods

4.1 General approach

In order to analyze each pixel separately we disassembled the time series of NDVI, PRC and LST images into a number of time series for each pixel. So we had 184 x 115 = 21160 (by the number of pixels) sequences of numeric values (time series vectors) for each of the three variables (Fig. 2 – Input). Each time series vector had 168 values (14 years of monthly observations). Then we decomposed each pixel's time series vector of each variable (NDVI, PRC and LST) into trend and seasonal components, omitting the remainder component. This is described in "4.2 Time series decomposition" section. Thus for each pixel of each variable we got trend and seasonal temporal components (Fig. 2 – Step 1). The trend components were used for the interannual assessment, and the seasonal components were used for the intra-annual assessment.

Then we conducted correlation analysis of trend and seasonal components respectively between NDVI and LST, and between NDVI and PRC at different lags (Fig.2 – Step 2). We identified the lags of maximum, minimum, maximum of absolute value and minimum of absolute value (Max, Min, AbsMax, AbsMin) correlation coefficients for each pixel (Fig. 2 – Step 4). This is detailed in the "4.3 Correlation analysis" section.

To understand how much of NDVI variation is explained by PRC and LST we conducted least squares regression analysis. We used NDVI trend and seasonal components as dependent variables and PRC and LST trend and seasonal components respectively as predictors. The predictors were shifted against NDVI time series for the lags of their AbsMax correlation to account for the delayed reaction (Fig. 2 – Step 3). Thus, for each pixel we have got the coefficient of determination (adjusted R^2) (Miles 2014) by climatic factors. This is described in more details in the "4.4 Coefficient of determination" section.

Then the trend and seasonal Max, Min, AbsMax, AbsMin images together with R^2 image and digital elevation model (DEM) were exposed to k-mean cluster analysis (Fig. 2 – Step 5). Thus we have got 5 spatial clusters with similar NDVI and climate temporal patterns considering elevation. Then we spatially averaged the trend and seasonal components of all the pixels within each cluster for each variable to see the general behavior of NDVI, precipitation and temperature in each cluster. These steps are described in the "4.5 Cluster analysis" section.

4.2 Time series decomposition

We approached the raster time series of NDVI, LST and PRC as a number of cross-correlated time series vectors (for each pixel) considering each vector independently from the others. We split the raster time series of NDVI, LST and PRC into a number of series of consecutive numeric values (vectors) –

Tab. 1: STL settings used for time series decomposition

Parameter	Value	Description
s.window	„periodic"	The loess window for seasonal extraction.
s.degree	1	Degree of locally-fitted polynomial in seasonal extraction.
t.window	36	The span (in lags) of the loess window for trend extraction.
t.degree	1	Degree of locally-fitted polynomial in trend extraction.
l.window	NULL	The span (in lags) of the loess window of the low-pass filter used for each subseries. Defaults to the smallest odd integer greater than or equal to the frequency of time series (i.e. 13).
l.degree	1	Degree of locally-fitted polynomial for the subseries low-pass filter.
robust	TRUE	Logical indicating if robust fitting be used in the loess procedure.
inner	2	Integer; the number of 'inner' (backfitting) iterations.
outer	1	Integer; the number of 'outer' robustness iterations.
na.action	na.omit	Action on missing values.

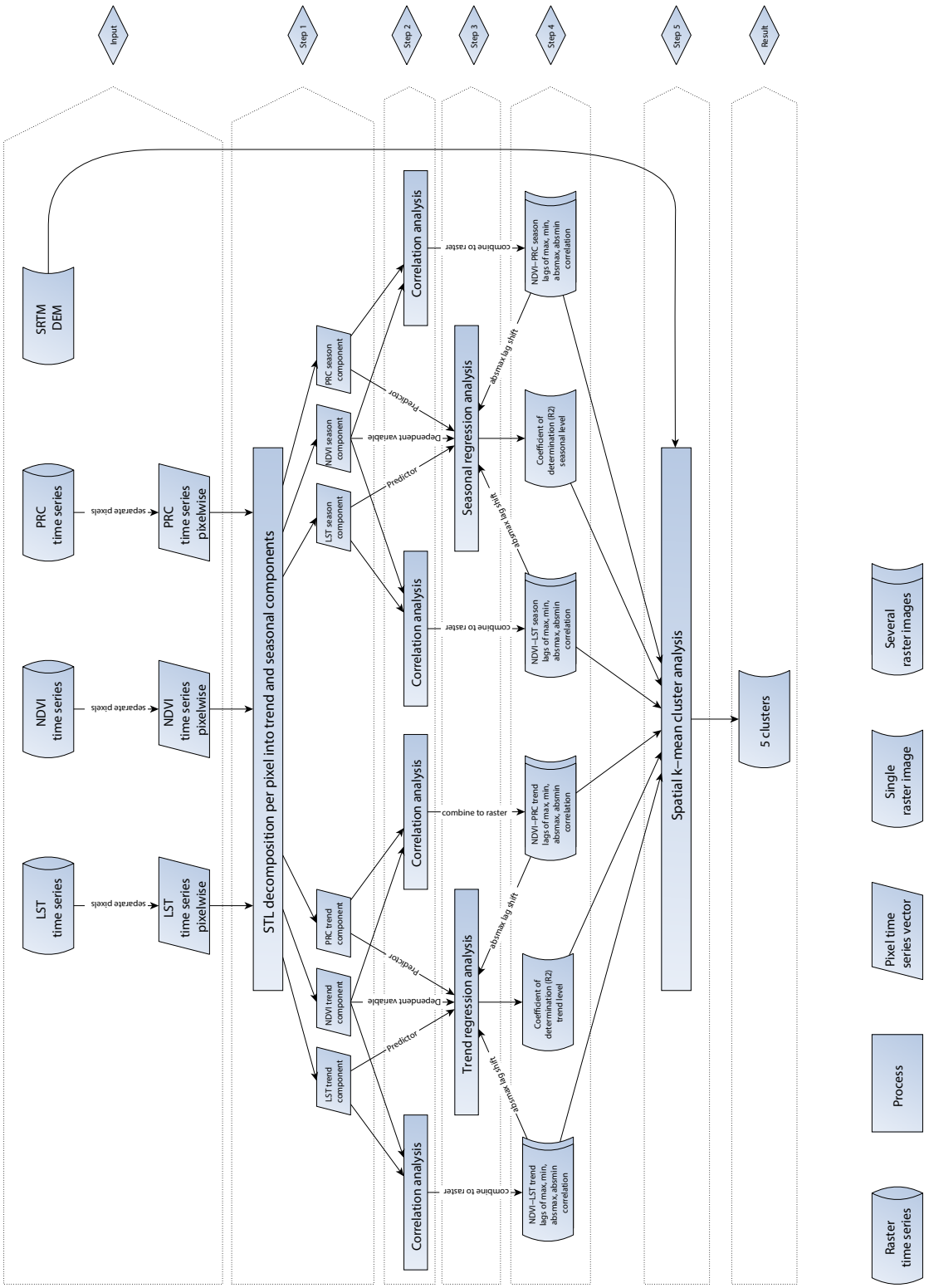

Fig. 2: Workflow chart

one for each pixel, thus we got 21160 vectors (by the number of pixels) of monthly values of NDVI, LST and PRC for the period of 14 years (2000-2013) (Fig. 2 – Input).

Then each time series vector was decomposed to seasonal (intra-annual), trend (interannual) and remainder (error) components (also vectors) using *stl* function (Cleveland et al. 1990) (Tab. 1) of *stats* package of R (R CORE TEAM 2016) (Fig. 2 – Step 1). STL decomposes time series into trend, seasonal and remainder components, which are the summands of the initial time series. The method is easy to implement, provides flexibility in choosing the amount of trend and seasonal variations, handles missing data and is robust against the outliers (Cleveland et al. 1990). STL is based on a sequence of smoothing operations mainly based on locally-weighted regression or *loess* (Cleveland and Devlin 1988; Cleveland et al. 1988).

This resulted in production of trend, seasonal and remainder components (vectors) for each pixel of each variable (Fig. 2 – Step 1). The remainder vectors were omitted from further analysis, thus we have got 21160 (by the number of pixels) trend and seasonal vectors for NDVI, LST and PRC.

4.3 Correlation analysis

We conducted cross-correlation analysis of the trend component vectors of NDVI with those of PRC and LST with different lags. The seasonal component vectors of NDVI were also correlated with respective vectors of PRC and LST (Fig. 2 – Step 2). In case of seasonal components correlation analysis, we looked at lags of up to 6 months, in case of the trend components we used up to 24 months lags. As a result we have got vectors of trend and seasonal components' correlation coefficients at different lags between NDVI and PRC and between NDVI and LST for each pixel. This way we could see how strongly NDVI correlates with PRC and LST on trend and seasonal scales with different lags in each pixel.

Then we identified at which lags NDVI had the Max, Min, AbsMax and AbsMin correlations with PRC and LST on trend and seasonal scales. These values we assembled into raster images of lags of Max, Min, AbsMax and AbsMin correlations of trend and seasonal components (Fig. 2 – Step 4). This provides information of speed and sign of NDVI reaction to precipitation and temperature on seasonal (intra-annual) and trend (interannual) scales.

4.4 Coefficient of determination

To estimate the coefficient of NDVI determination by the climatic factors on the interannual scale we conducted a regression analysis with NDVI trend components being the dependent variable and PRC and LST trend components as predictors. For the intra-annual scale we did the same with the seasonal components of the variables. The predictors were taken at the lags of their AbsMax correlation with NDVI (Fig. 2 – Step 3). The regression analysis was conducted on the pixel basis, i.e. each pixel's NDVI was predicted with its PRC and LST values taken at their respective AbsMax correlation lag. The following equation was used for the regression analysis in Fig. 2 – Step 3:

$$NDVI_t = a * PRC_{t-i} + b * LST_{t-j} + c \quad (1)$$

Where:

$NDVI_t$ – normalized difference vegetation index at lag $t = 0$ (current observation), PRC_{t-i} – precipitation i lags earlier, LST_{t-j} – land surface temperature j lags earlier, a, b, c – first, second and third polynomial coefficients of the regression equation, i – lag of AbsMax correlation of *NDVI* and *PRC*, j – lag of AbsMax correlation of *NDVI* and *LST*.

Based on the regression analysis we calculated the coefficient of determination, which was the adjusted R^2 (Miles 2014). This was done both for trend and seasonal components of each pixel separately (i.e. each pixel had individual lag shifts for each predictor), thus we could see to which extent the NDVI variations were conditioned by precipitation and temperature variations, considering the predictor- and pixel-specific reaction time, which was the lag of AbsMax correlation with predictors (Fig. 2 – Step 4).

4.5 Cluster analysis

The images of lags of Max, Min, AbsMax and AbsMin correlation coefficients, together with the images of R^2 on both trend and seasonal scales and digital elevation model (DEM) were exposed to k-mean (Rubin 1967) grid cluster analysis (Fig. 2 – Step 5). As a result we have got 5 spatial clusters with different temporal patterns of NDVI, LST and PRC. We have spatially averaged all the pixels within each cluster to see the temporal pattern of vegetation and climate interaction in each of them.

5 Results

The correlation analysis resulted in 32 images, which represent Max, Min, AbsMax and AbsMin correlation coefficients of NDVI correlation with PRC and LST, together with their lags and on trend and seasonal scales (Fig. 2 – Step 4). The representation and discussion of all the images would be too overwhelming, so we present the AbsMax images and their respective lags (Fig. 3). These images (Fig. 3) indicate the different signs of NDVI correlation with PRC and LST and different lags, at which they occur. In general NDVI on low flat areas indicate positive correlation with PRC and negative with LST, whereas highlands indicate the opposite (Fig. 3). Since the maximum of absolute value function was looking for correlation coefficients with lags of up to 6 months on the seasonal scale and 24 months on the trend scale, the weaker correlations with other signs could be covered with the stronger correlations with

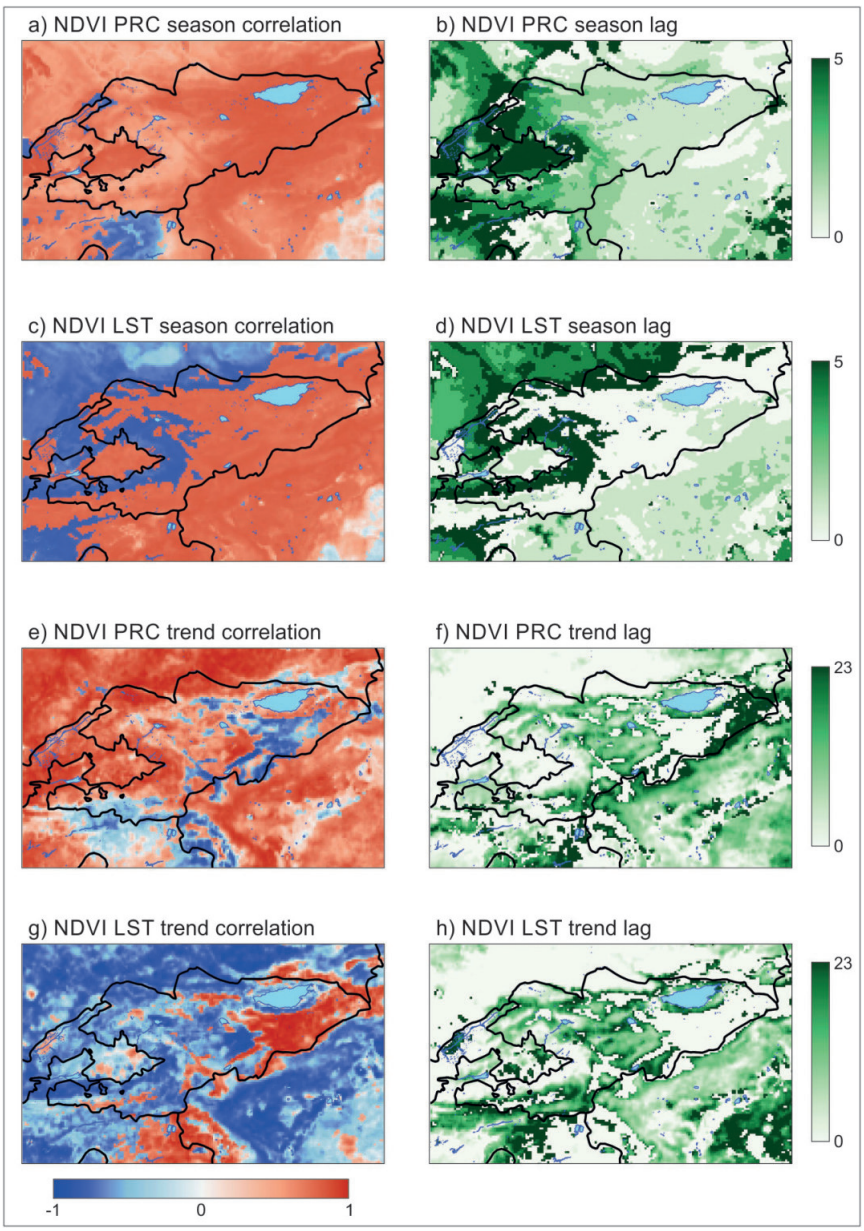

Fig. 3: The maps of AbsMax correlation coefficients (left column) and their respective lags in months (right column)

the opposite sign. These interactions were captured with other extrema functions and the cluster analysis (Fig. 2 – Step 5) is to decrease the dimensionality of results and present them more comprehensively.

The resulting 5 clusters followed the pattern of horizontal temperature and precipitation flow as well as altitudinal gradients (Fig. 4). They indicate the spatial pattern of inter- and intra-annual variations of vegetation and climatic factors. None of the clusters repeat any other with regards to annual mean of precipitation, temperature and NDVI (Fig. 5).

The cluster 1 is basically the flat lands in Kazakhstan and China representing dry deserts or desert-steppes (Fig. 4). In absolute values the mean monthly precipitation level in this cluster is about 25 mm, mean monthly NDVI is 0.23 and mean monthly LST is 24°C (Fig. 5). The seasonal component of NDVI indicates a strong positive correlation with precipitation (Tab. 2) and the seasonal flow of NDVI closely complies with the seasonal flow of PRC with a month lag (Fig. 6c), meaning a delayed reaction of NDVI to precipitation (Fig. 6a). NDVI also indicates a week positive immediate correlation with LST and a negative correlation with 4 months lag (Fig. 6b). This indicates that temperature is a promoting as well as a limiting factor for vegetation development. The summer, which is the seasonal maximum of temperature, coincides with seasonal minimum of NDVI and precipitation, which results in an arid landscape. Vegetation booms in spring and is depressed by high temperatures and low precipitation levels in summer. This cluster has the highest monthly temperature among the other clusters (Fig. 5). On the trend scale, positive correlation with precipitation and negative correlation with temperature is obvious (Fig. 6d, e). The trend component curves of NDVI and precipitation almost entirely match with each other, opposed by the temperature curve (Fig. 6f). About 61 % of NDVI seasonal variation and about 64 % of its interannual variation are explained by PRC and LST (Tab. 2).

The cluster 2 is mainly low mountains in Toktogul, Fergana and Chui valleys, which are foothills of Fergana, Chatkal and Kyrgyz Ala-Too ranges (Fig. 4). The area has dense networks of rivers and irrigation channels, it is mainly used as crop fields or lowland pastures. On the seasonal scale, NDVI indicates positive correlations with precipitation with a lag of 4 months (Fig. 7a) and immediate positive correlation with temperature (Fig. 7b). NDVI curve follows the temperature curve and is also conditioned by the precipitation

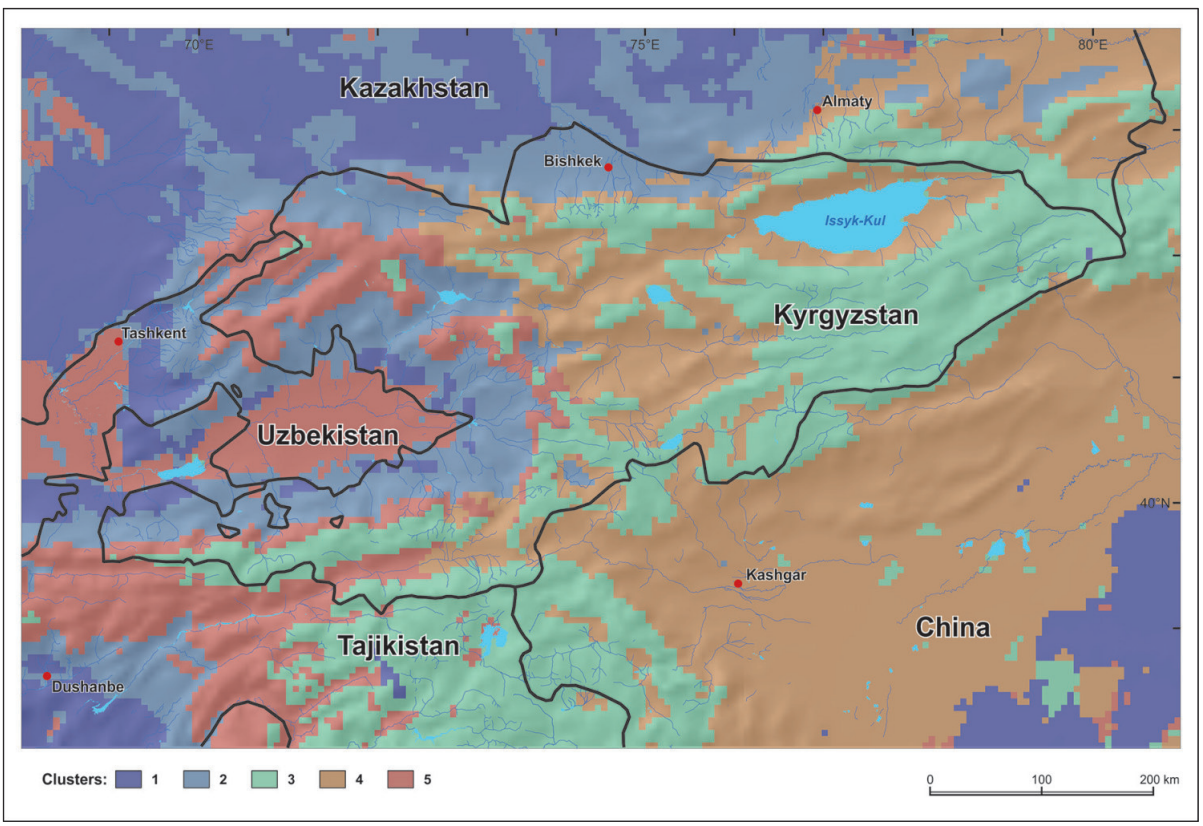

Fig. 4: Spatial clusters of vegetation-climate interactions

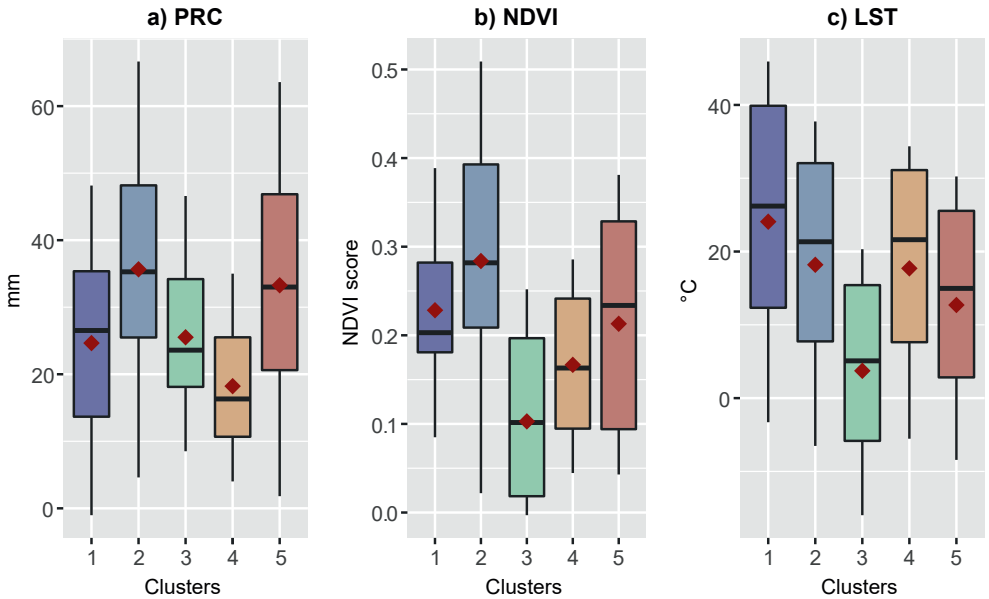

Fig. 5: Cluster spatially averaged values (boxplots) red dots represent mean values

curve (Fig. 7c). NDVI does not drop immediately with the precipitation in summer; however, high temperatures do depress vegetation. On the trend scale, NDVI indicates a strong positive correlation with precipitation and strong negative correlation with temperature (Tab. 2). NDVI trend curve follows very closely the precipitation curve and is opposed by the temperature curve (Fig. 7f). This cluster has the highest monthly mean precipitation level (36 mm per month) and highest mean NDVI (0.28) with a monthly mean temperature of about 18°C (Fig. 5). About 81 % of the seasonal variation and 68 % of the trend variation of NDVI are explained by the climatic factors (Tab. 2).

The cluster 3 represents the areas of highland tundra which are used as winter pastures (Fig. 4). These areas comprise highland plains or tops of ridges with very sparse and low vegetation. Here, NDVI on the seasonal scale shows strong positive no lag correlation with temperature, and strong positive correlation with precipitation with 1-2 months lag (Fig. 8a, b). The NDVI curve basically follows the temperature curve (Fig. 8c), the peak of precipitation curve in May supports NDVI development, which peaks later in July. On the trend scale, NDVI shows a strong negative correlation with precipitation and positive correlation with temperature (Tab. 2), which is different to the other clusters. NDVI trend curve follows closely the temperature curve (Fig. 8f) and precipitation curve lags after NDVI, which is illustrated by the cross correlation function (Fig. 8d). In absolute terms, this cluster has the lowest temperature and NDVI. The mean monthly temperature is about 4°C, NDVI averages at 0.1 and precipitation at 26 mm per month (Fig. 5). About 88 % of the seasonal and about 58 % of the trend NDVI variations are determined by the climatic factors (Tab. 2).

Tab. 2: Cluster characteristics – AbsMax correlation coefficients (CC) and their lags (Lag), mean adjusted R2 of seasonal and trend components for each cluster

Cluster	NDVI, PRC s		NDVI, LST s		NDVI, PRC t		NDVI, LST t		R^2	
	CC	Lag	CC	Lag	CC	Lag	CC	Lag	s	t
Cluster 1	0.61	1	-0.82	4	0.94	0	-0.76	0	0.61	0.64
Cluster 2	0.59	4	0.85	0	0.94	0	-0.79	0	0.81	0.68
Cluster 3	0.92	1	0.93	0	-0.62	0	0.75	0	0.88	0.58
Cluster 4	0.96	1	0.94	0	0.67	10	-0.70	13	0.87	0.60
Cluster 5	0.85	5	0.98	0	0.72	6	-0.55	9	0.89	0.52

s – seasonal, t – trend

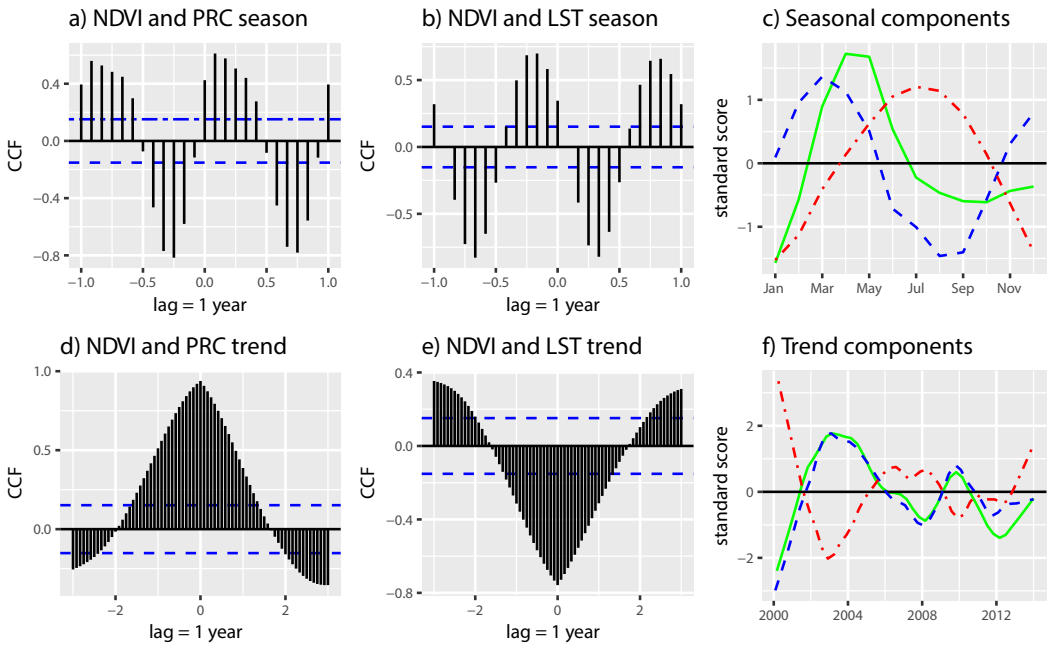

Fig. 6: Cluster 1 seasonal and trend components lagged cross-correlation (for time=*t* and lag=*f* the correlation coefficient is calculated between $NDVI_{t+f}$ and PRC_t or LST_t), and their standard scores: solid green – NDVI, dot-dashed red – LST, dashed blue – PRC

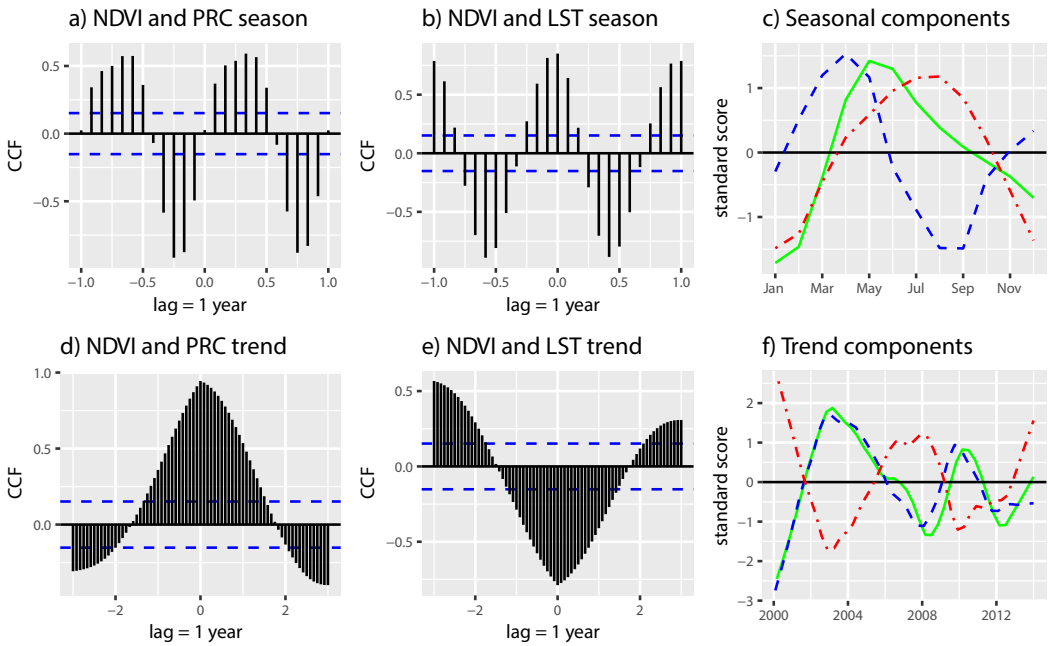

Fig. 7: Cluster 2 seasonal and trend components lagged cross-correlation (for time=*t* and lag=*f* the correlation coefficient is calculated between $NDVI_{t+f}$ and PRC_t or LST_t), and their standard scores: solid green – NDVI, dot-dashed red – LST, dashed blue – PRC

The cluster 4 is mainly dry plains or intermontane depressions (Fig. 4). These areas have the least precipitation amount among the clusters (Fig. 5), because they occur in the precipitation shadows of Fergana and Kokshal-Too ranges. Here NDVI, PRC and LST seasonal curves almost coincide with each other (Fig. 9c) and have strong positive correlation with 0 to 1 lag difference (Fig. 8a, b). On the inter-

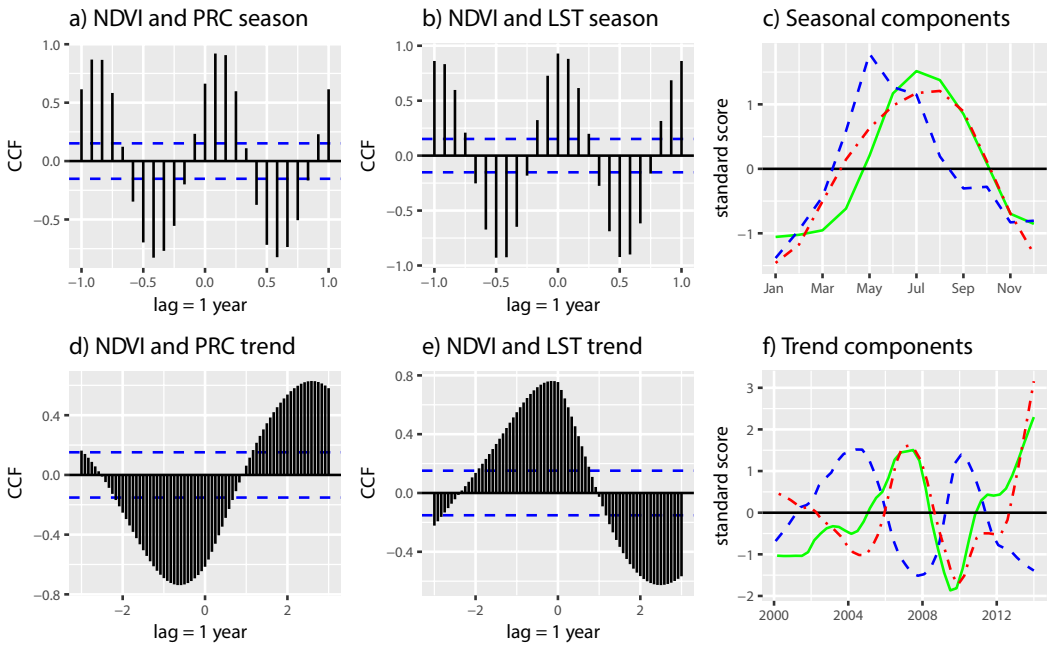

Fig. 8: Cluster 3 seasonal and trend components lagged cross-correlation (for time=*t* and lag=*f* the correlation coefficient is calculated between $NDVI_{t+f}$ and PRC_t or LST_t), and their standard scores: solid green – NDVI, dot-dashed red – LST, dashed blue – PRC

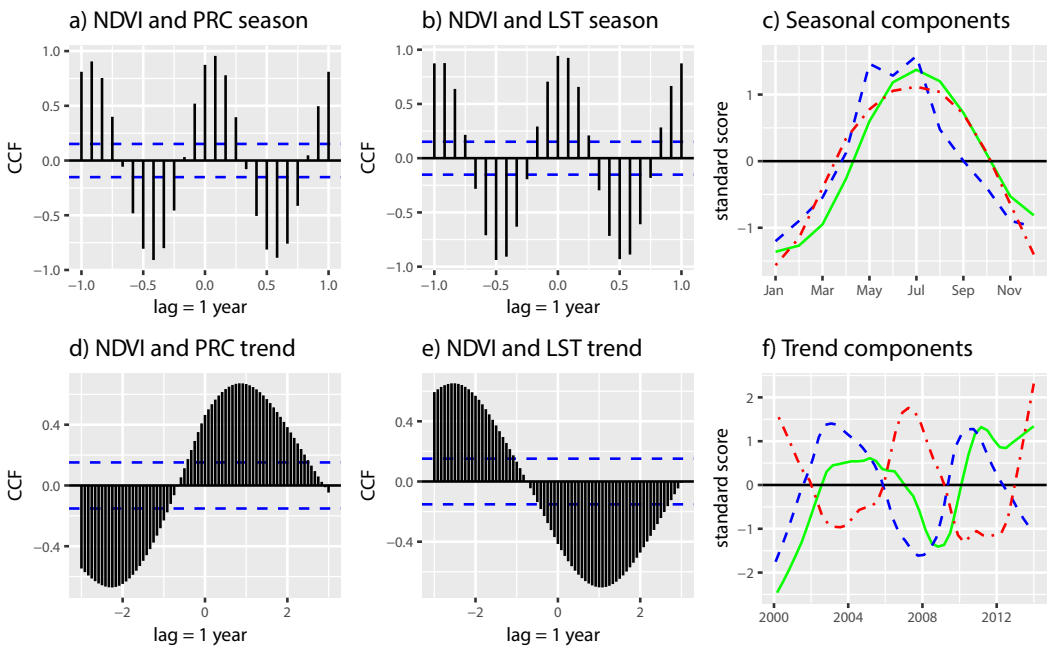

Fig. 9: Cluster 4 seasonal and trend components lagged cross-correlation (for time=*t* and lag=*f* the correlation coefficient is calculated between $NDVI_{t+f}$ and PRC_t or LST_t), and their standard scores: solid green – NDVI, dot-dashed red – LST, dashed blue – PRC

annual scale, NDVI indicates a strong positive correlation with PRC and a strong negative correlation with LST with about one year lag (Fig. 9d, e). This is also caused by the rain shadow effect of the ridges, surrounding the cluster areas. Mean monthly precipitation level is about 18 mm, temperature is 18°C and NDVI score is 0.17 (Fig. 5). This cluster has the greatest lag of the trend components correlation with

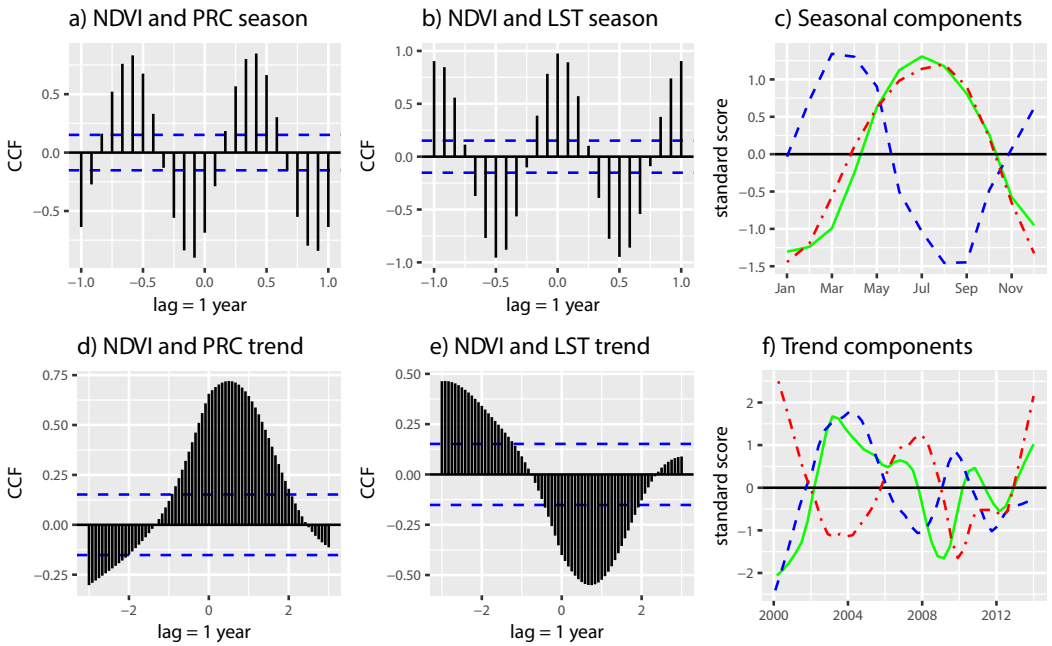

Fig. 10: Cluster 5 seasonal and trend components lagged cross-correlation (for time=*t* and lag=*f* the correlation coefficient is calculated between $NDVI_{t+f}$ and PRC_t or LST_t), and their standard scores: solid green – NDVI, dot-dashed red – LST, dashed blue – PRC

about 87 % and 60 % of NDVI seasonal and trend variations, respectively, being determined by the climatic factors (Tab. 2).

The cluster 5 occupies Fergana valley and some slopes of Fergana, Chatkal and Alai ranges (Fig. 4). These are the areas with one of the highest precipitation levels (Fig. 5). This is a very active agricultural region with developed irrigation network. On the seasonal scale, the NDVI curve follows the temperature curve very closely, indicating a strong positive correlation without a lag (Fig. 10b), whereas precipitation indicates positive correlation with a lag of 5 months (Fig. 10a). On Fig. 10a we can see an artificial negative correlation between NDVI and PRC at lag 0 and a real positive at 6 months lag; this is caused by the system of artificial irrigation, which stocks rain water in spring and provides it in summer. This makes the NDVI peak to shift to summer (Fig. 10c), when vegetation is provided with solar heat and irrigation water, collected from spring rains. The interannual NDVI and precipitation indicate a strong positive correlation and their curves follow each other, whereas temperature has negative correlation with NDVI (Fig. 10d, e). The monthly mean precipitation level here is about 33 mm, mean NDVI is 0.21 and the mean monthly temperature is 13°C (Fig. 5). About 89 % of NDVI seasonal and 52 % of the interannual variations are determined by the climatic factors (Tab. 2).

The coefficient of determination (adjusted R^2) derived from the regression analysis of the seasonal components indicates vast areas to be strongly conditioned by precipitation and temperature. The mean coefficient of determination of all the pixels is 0.82 and standard deviation equals to 0.17. Only the areas in the north-west and south-east, which are Muyun-Kum and Taklamakan deserts in Kazakhstan and China respectively, and Khan-Tengri glaciers, indicate low coefficients of determination (Fig. 11). The Fergana valley with developed agriculture and irrigation system is also less controlled by the climatic factors.

The trend component of NDVI indicates less determination by precipitation and temperature. The mean is 0.60 and standard deviation equals to 0.20. The areas with the least R^2 are the tops of Fergana, Chatkal and Alai ridges, Khan-Tengri, Suusamyr valley as well as At-Bashy, Kemin and Son-Kul valleys (Fig. 12). The plains in Kazakhstan and China, highlands in Inner Tian-Shan and parts of Fergana valley in Tajikistan show high coefficients of determination. These areas are expected to be affected the most in case of temperature and precipitation trend change.

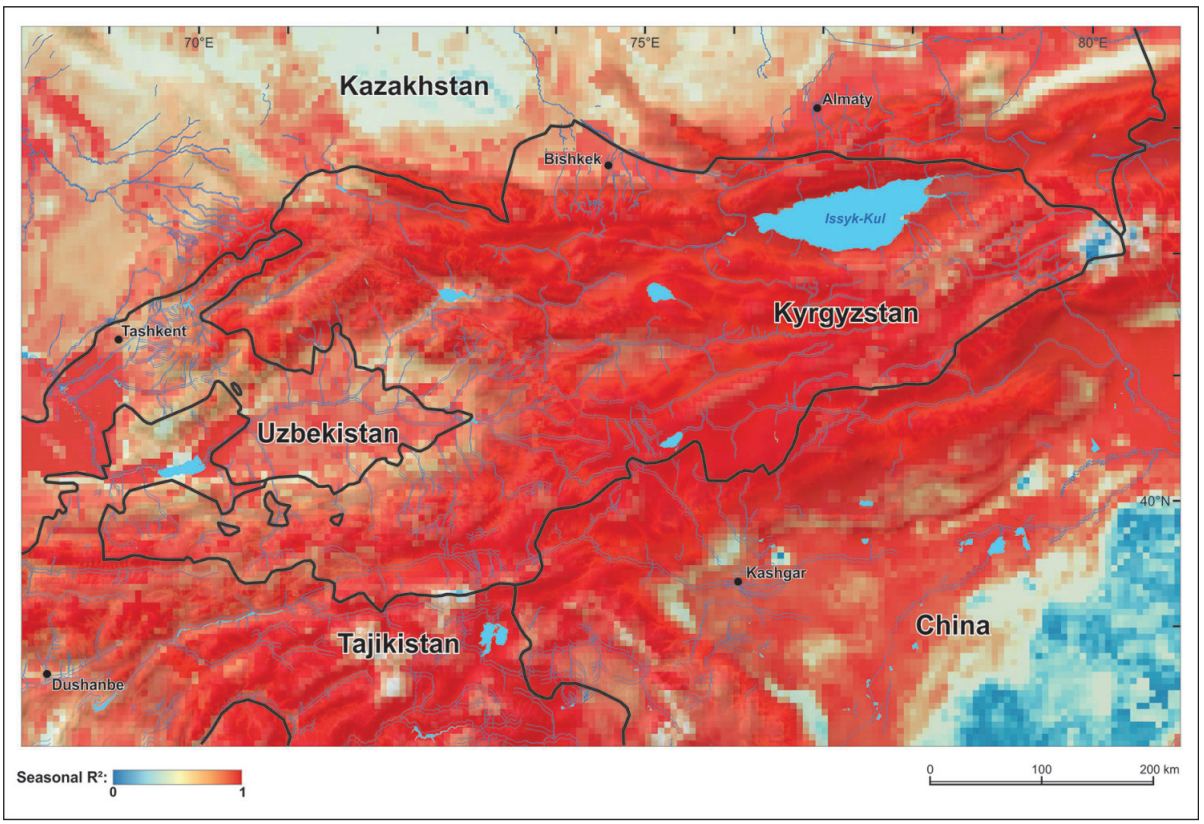

Fig. 11: Coefficient of determination (adjusted R^2) of NDVI seasonal component (indicates to which extent NDVI seasonal variation is determined by precipitation and temperature seasonal variations)

6 Discussion

The 5 clusters identified in this study indicate 5 zones with different patterns of vegetation and climate interaction. The zones have different seasonal flow of NDVI, temperature and precipitation as well as different trends of the variables. On the seasonal scale, all the clusters have positive NDVI correlations with precipitation and temperature, except for cluster 1, which has negative correlation with temperature (Tab. 2). On the trend scale, NDVI in all the clusters has positive correlation with precipitation and a negative with temperature, except for cluster 3, where it is opposite.

In general, both PRC and LST are the promoting factors for vegetation development on the seasonal scale (Tab. 2). Only in clusters 1 and 2 vegetation is boosted by temperature in spring and depressed by it in summer (Figs. 6c, 7c). These clusters are deserts and plains in Kazakhstan and China, and piedmonts of Fergana and Chatkal ridges. Similar results were reported by Propastin et al. (2008a) and Yin et al. (2016), who identified positive correlation between NDVI and temperature in spring and negative correlation in summer for different vegetation types in Central Asia. Both temperature and precipitation can be promoting as well as limiting factors of plant growth if they deviate considerably from their optimal values and timing, which varies with elevation, terrain and other natural conditions.

Temperature seasonal distribution stays constant across the clusters, because generally summers are warm and winters are cold. However, the seasonal distribution of precipitation and its absolute values varies drastically; which conditions vegetation temporal behavior and makes the clusters different. The seasonal maxima of NDVI, temperature and precipitation move in geographical space as the seasons change. Precipitation maximum flows from northwest to south-east over the year cycle. The temperature maximum moves from low valleys to the ridge tops from spring to winter. NDVI maximum basically follows behind the precipitation maximum, suggesting that vegetation development in the region is conditioned more by precipitation than by temperature.

On the trend scale, precipitation appears to be the promoting factor, whereas temperature is always the limiting factor for vegetation develop-

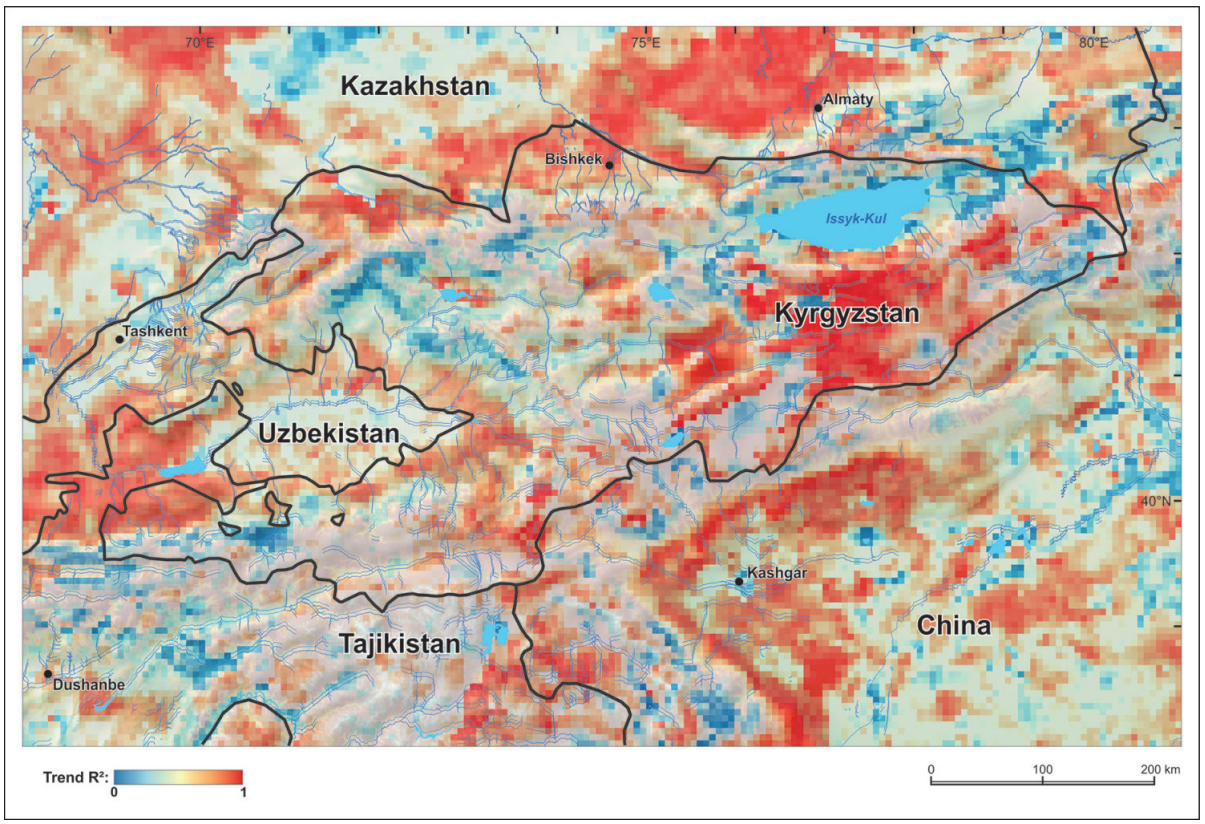

Fig. 12: Coefficient of determination (adjusted R^2) of NDVI trend component (indicates to which extent NDVI trend variation is determined by precipitation and temperature trend variations)

ment (Tab. 2). Thus, an increase in precipitation will promote vegetation, and increasing temperatures will limit it. This indicates the general aridity of the region, similar findings are reported by YIN et al. (2016). Cluster 3 is the only exception indicating the opposite. This cluster occupies the areas of highland plains and ridge tops. These areas usually have low temperatures and significant water deposits, so precipitation in the form of snow retards the vegetation development, but higher temperatures promote its growth. This cluster has the lowest mean annual NDVI and temperature and about the average precipitation (Fig. 5), so not the lack of moisture and high temperature, but lots of snow and low temperature are the main limiting factors for vegetation development on the trend scale. The cluster 3 is the only case where NDVI variations precede those of precipitation and temperature on the trend scale (Figs. 8d, e). This suggests that vegetation has an impact on local microclimate. We can suppose that developing vegetation cover decreases evapotranspiration and albedo in the area, which in turn limits precipitation and increases temperature.

Clusters 2 and 5 show close mean monthly values (Fig. 5); they are close geographically as well (Fig. 4). However, seasonal distribution of NDVI and correlation of trend components are different (Figs. 7, 10). Similar seasonal distribution of precipitation and temperature for cluster 5 was reported by LIOUBIMTSEVA et al. (2005) and by GESSNER et al. (2013). At the same time the clusters with similar seasonal flow indicate different absolute values, like clusters 3 and 4. This clearly shows a great regional variability of the climate-vegetation system and importance of their discrimination. It is also important to consider not only the absolute values or seasonal flows of NDVI, LST and PRC, but both these factors together with the reaction lag.

The major climate analysis of Kyrgyzstan was conducted by ADYSHEV et al. (1987). This climate classification was developed from annual sums of temperature and precipitation as well as their seasonal distribution and elevation, based on meteorological observations since 1881 (GIDROMET SSSR et al. 1967) and is broadly applied in the country. Our clusters 1, 2 and 5 correspond to "valley and foothill" climatic belt according to the classification by

Adyshev et al. (1987). Cluster 4 corresponds to the "midland" climatic belt, and cluster 3 corresponds to "highland" and "nival" climatic belts of the same classification (Adyshev et al. 1987). Thus our study discriminated 3 additional classes within the "valley and foothill" class and combined the "highland" and "nival" classes into one. The classification by Adyshev et al. (1987) was based on climatic and terrain variables, whereas our study uses the vegetation component, which makes it more useful with regards to management of natural resources and climate change adaptation.

Lioubimtseva and Henebry (2009) and Hijioka et al. (2014) predicted aridity increase in Central Asia in the coming decades. The summers will be hotter and dryer, and winters will have more precipitation. These will shift the temperature and precipitation seasonal curve and change the trend, which will have corresponding impacts on vegetation. The fact that almost the entire research area has high coefficient of determination scores on the seasonal scale (Fig. 11) indicates that seasonally the vegetation is greatly dependent on climatic factors. Only the arid lands and permanent glaciers indicate little to no NDVI seasonal variation determination by the climatic factors (Fig. 11). These are the areas without much vegetation, which would not normally respond to temperature and moisture variations. In general, on the seasonal scale pastures and forests indicate the highest coefficient of determination, the agricultural areas show the medium, and the areas without vegetation have the lowest coefficient of determination. Propastin et al. (2007) also indicate decrease of correlation between NDVI and climatic factors in different ecosystems as the proportion of grass species shrinks.

On the trend scale, the pattern of determination is more complex and reflects both the areas without vegetation and with dense and stable vegetation cover (Fig. 12). The areas with average vegetation cover indicate the highest coefficient of determination, whereas the areas with either no vegetation or dense vegetation cover indicate very low coefficient of determination. This is because bare areas have nothing to react to climatic factors, and dense vegetation is robust against interannual climate fluctuations. These areas are expected to be more resistant against climate change, whereas the areas with average vegetation cover will be mostly affected by climate change. For example vegetation on some elevated areas like Fergana, Alai and Kyrgyz ridges as well as Pamir mountains are not conditioned by the climatic factors (Fig. 12), which is in agreement with Hu et al. (2014), who found negative correlation between temperature increase and elevation. Chui, Talas, Ili and Fergana valleys are the regions with intensive agriculture; however the trend coefficient of determination in Fergana valley is considerably lower (Fig. 12), suggesting it has more efficient irrigation system. The areas with high coefficient of determination, like eastern part of Inner Tian-Shan, Chui and Talas valleys, Karatau ridge and Ili depression as well as Turkestan ridge foothills, Syr-Daria river valley, and Kyzyl-Suu region in China are expected to suffer most under the conditions of changing climate.

The vegetation response to precipitation change comprises 1-5 months lag, whereas that of temperature is 0 for most of clusters (Tab. 2). Many global-scale studies indicate an average lag of 1-2 month of vegetation reaction to precipitation (Potter and Brooks 1998; Schultz and Halpert 2007). Gurgel and Ferreira (2003) conducted lagged correlation analysis of 3 NDVI time series principal components and precipitation principal components for the entire area of Brazil. They identified that different vegetation types had 0-3 months response time to precipitation. Gessner et al. (2013) found 1-3 months lag between precipitation change and vegetation reaction in Central Asia. Propastin et al. (2007) identified a lag of 0-60 days between precipitation and NDVI and no lag between temperature and NDVI with temperature contributing the most to NDVI variations in central Kazakhstan. All these findings are in agreement with the results of our research (Tab. 2).

Several studies (Propastin et al. 2008a; Zhao et al. 2011; Kariyeva and Van Leeuwen 2011; Mohammat et al. 2013; Zhang et al. 2013; Du et al. 2015; Eckert et al. 2015; Yin et al. 2016) used spatial and temporal averaging of NDVI and climatic factors to identify their inter-annual relations and least squares to find the temporal trend. The spatial averaging was conducted within different vegetation classes and temporal averaging was conducted within spring, summer, autumn and these three seasons together. However these approaches do not consider seasonality, some of them – delayed reactions and do not distinguish between seasonal and trend components. They assume a positive correlation between NDVI and precipitation, which prevents complex assessments of time series data (e.g. Fig. 3). Spatial averaging prevents from identification of fine scale patterns and introduces bias by dividing the study area into predetermined sectors. Instead, Gessner et al. (2013) used lagged correlation analysis between NDVI and precipitation time series on a pixel basis, considering accumulation periods, which allowed for identification of complex interactions.

Our research was based on decomposition of time series of raster data into trend and seasonal components on per-pixel basis and analysis of the components separately. This approach allows for separation of inter-annual and intra-annual behavior of the variables and solves the data stationarity issue. At the same time the pixel-level discretization of the time-series helps to reduce the impact of spatial variability of other unconsidered factors like soil, elevation, exposure etc. Identification of pixel-specific NDVI reaction to temperature and precipitation (Fig. 3) and then grouping them into k-mean clusters with similar behavior (Fig. 4) reduces the bias and helps to identify the natural patterns.

The uncertainties of the methods used in this study include the phenological autocorrelation of NDVI, which can be falsely attributed to precipitation or temperature variations. Temperature and precipitation as predictors can have significant correlation, which can affect the model accuracy. And the fact that predictors have positive effect within a certain value window and otherwise outside of that is not considered in the model. However these issues are addressed by taking the predictors at the lags of their AbsMax correlation with NDVI, not with each other. Snow and rain are also mixed in the precipitation variable which also can potentially lead to errors as snow cover can artificially decrease NDVI score. Also, snow precipitation makes moisture available to vegetation at the time of melting, not at the time of falling, which is not considered in the seasonal analysis, but luckily in our case winter is rarely the season of maximum precipitation. Snow accumulation provides more water in summer with meltwater providing higher discharge in streams, which can induce a delayed effect in the areas downstream. Rivers and accumulated moisture are also not considered here. Different soil types can have an effect. However, using the standard scores of the variables and per-pixel approach can decrease this limitation.

7 Conclusion

We applied time series decomposition with *loess* to raster time series of vegetation, precipitation and temperature on pixel basis, followed by correlation analyses of the seasonal and trend components of the variables in each pixel. We did not assume any patterns prior to the analysis, neither with regard to spatial variations, nor with regard to temporal response to avoid any bias. Thus the data were analyzed at the finest scale possible and the results were subjected to k-means cluster analysis to identify the areas of climate-vegetation interaction similarity.

The results indicate that vegetation can be both positively or negatively affected by the climatic factors, which can result in a complicated pattern of climate-vegetation interactions. Thus vegetation response sign and lag should not be assumed by the methods used. Spatial variability of climate-vegetation interaction can be great so any kind of spatial averaging prior to the analysis should be avoided and all the pixels should be treated independently from each other unless a more sophisticated method, accounting for such interactions is applied. The seasonal averaging of temporarily explicit data should also be avoided, as it can prevent the identification of temporal patterns. Instead, seasonal decomposition of signal and correlation analysis with lags should be applied to assess seasonal and interannual interactions.

The resulting climate-vegetation patterns indicate great variability over the relatively small study area. This is presumably conditioned by complex terrain and mixed influence of neighboring arid areas and humid air masses, coming from the west. The vegetation communities in the region indicate vulnerability to temperature and precipitation trend change as they are conditioned by these factors. In the case of seasonality change of climatic factors most of the study area will be greatly affected, however, further modelling is needed to understand these interactions. The methodical approach, used in this study, can easily be transferred to other regions for assessment of climate change impacts on vegetation.

Acknowledgments

MODIS land surface temperature and vegetation index data are originally distributed by the Land Processes Distributed Arctive Archive Center (LP DAAC), located at the U.S. Geological Survey (USGS) Earth Resources Observation and Science (EROS) Center (lpdaac.usgs.gov), distributed in netCDF format by the Integrated Climate Data Center (ICDC, http://icdc.zmaw.de) University of Hamburg, Germany. We are thankful to the Integrated Climate Data Center, University of Hamburg, Germany and Dr. Stefan Kern for their continuous support. We are thankful to SRTM, OpenStreetMap and Natural Earth projects, whose data were used in maps. We also want to thank the reviewers for their valuable comments.

References

Adyshev; M.M.; Kashirin; F.T.; Umurzakov; S.U.; Almaev; T.M.; Voronina; A.F.; Grigorenko; P.G.; Dzhamgerchinov; B.D.; Zabirov; R.D.; Zinkova; Z.Y.; Izmailov; A.E.; Isabaeva; V.A.; Kravchenko; A.V.; Mamytov; A.M.; Makhrina; L.I.; Moldokulov; A.M.; Murzaev; E.M.; Otorbaev; K.O.; Popova; L.I.; Yar-Mukhamedov; G.K.; Yashina; V.V. and Chernova; L.I. (1987): Atlas Kirgizskoi SSR (vol. I) (in Russian). Moscow.

Borchardt, P.; Oldeland, J.; Ponsens, J. and Schickhoff, U. (2013): Plant functional traits match grazing gradient and vegetation patterns on mountain pastures in SW Kyrgyzstan. In: Phytocoenologia 43, 171–181. https://doi.org/10.1127/0340-269X/2013/0043-0542

Borchardt, P.; Schickhoff, U.; Scheitweiler, S. and Kulikov, M. (2011): Mountain pastures and grasslands in the SW Tien Shan, Kyrgyzstan - Floristic patterns, environmental gradients, phytogeography, and grazing impact. In: Journal of Mountain Science 8, 363–373. https://doi.org/10.1007/s11629-011-2121-8

Cao, L.; Xu, J.; Chen, Y.; Li, W.; Yang, Y.; Hong, Y. and Li, Z. (2013): Understanding the dynamic coupling between vegetation cover and climatic factors in a semiarid region-a case study of Inner Mongolia, China. In: Ecohydrology 6, 917–926. https://doi.org/10.1002/eco.1245

Christensen, J.H.; Hewitson, B.; Busuioc, A.; Chen, A.; X. Gao, I.H.; Jones, R.; Kolli, R.K.; Kwon, W.-T.; Laprise, R.; Rueda, V.M.; Mearns, L.; Menéndez, C.G.; Räisänen, J.; Rinke, A.; Sarr, A. and Whetton, P. (2007): Regional Climate Projections. In: Solomon, S., Qin, D., Manning, M., Chen, Z., Marquis, M., Averyt, K. B., Tignor, M. and Mille, H. L. (eds.): Climate Change 2007: The Physical Science Basis. Contribution of Working Group I to the Fourth Assessment Report of the Intergovernmental Panel on Climate Change. Cambridge, United Kingdom and New York, NY, USA.

Cleveland, R. B.; Cleveland, W. S.; McRae, J. E. and Terpenning, I. (1990): STL: a seasonal-trend decomposition procedure based on loess. In: Journal of Official Statistics 6, 3–73.

Cleveland, W. S. and Devlin, S. J. (1988): Locally weighted regression: an approach to regression analysis by local fitting. In: Journal of the American Statistical Association 83, 596–610.

Cleveland, W. S.; Devlin, S. J. and Grosse, E. (1988): Regression by local fitting: methods, properties, and computational algorithms. In: Journal of econometrics 37, 87–114.

Conrad, O.; Bechtel, B.; Bock, M.; Dietrich, H.; Fischer, E.; Gerlitz, L.; Wehberg, J.; Wichmann, V. and Böhner, J. (2015): System for automated geoscientific analyses (SAGA) v. 2.1.4. In: Geoscientific Model Development 8, 1991–2007. https://doi.org/10.5194/gmd-8-1991-2015

Crewett, W. (2012): Improving the sustainability of pasture use in Kyrgyzstan. In: Mountain Research and Development 32, 267–274. https://doi.org/10.1659/MRD-JOURNAL-D-11-00128.1

de Beurs, K. M.; Wright, C. K. and Henebry, G. M. (2009): Dual scale trend analysis for evaluating climatic and anthropogenic effects on the vegetated land surface in Russia and Kazakhstan. In: Environmental Research Letters 4, 45012. https://doi.org/10.1088/1748-9326/4/4/045012

de Jong, R.; de Bruin, S.; de Wit, A.; Schaepman, M. E. and Dent, D. L. (2011): Analysis of monotonic greening and browning trends from global NDVI time-series. In: Remote Sensing of Environment 115, 692–702. https://doi.org/10.1016/j.rse.2010.10.011

de Jong, S. M. (1994): Derivation of vegetative variables from a Landsat TM image for modelling soil erosion. In: Earth Surface Processes and Landforms 19, 165–178. https://doi.org/10.1002/esp.3290190207

Dörre, A. and Borchardt, P. (2012): Changing systems, changing effects—pasture utilization in the post-Soviet transition. In: Mountain Research and Development 32, 313–323. https://doi.org/10.1659/MRD-JOURNAL-D-11-00132.1

Du, J.; Shu, J.; Yin, J.; Yuan, X.; Jiaerheng, A.; Xiong, S.; He, P. and Liu, W. (2015): Analysis on spatio-temporal trends and drivers in vegetation growth during recent decades in Xinjiang, China. In: International Journal of Applied Earth Observation and Geoinformation 38, 216–228. https://doi.org/10.1016/j.jag.2015.01.006

Dubovyk, O.; Landmann, T.; Dietz, A. and Menz, G. (2016): Quantifying the impacts of environmental factors on vegetation dynamics over climatic and management gradients of Central Asia. In: Remote Sensing 8, 600. https://doi.org/10.3390/rs8070600

Eckert, S.; Hüsler, F.; Liniger, H. and Hodel, E. (2015): Trend analysis of MODIS NDVI time series for detecting land degradation and regeneration in Mongolia. In: Journal of Arid Environments 113, 16–28. https://doi.org/10.1016/j.jaridenv.2014.09.001

Gessner, U.; Naeimi, V.; Klein, I.; Kuenzer, C.; Klein, D. and Dech, S. (2013): The relationship between precipitation anomalies and satellite-derived vegetation activity in Central Asia. In: Global and Planetary Change 110, 74–87. https://doi.org/10.1016/j.gloplacha.2012.09.007

Gidromet SSSR; G.U.G.S. pri S.M.; Gidromet KSSR; U.G.S. and Observatoriya; F.G. (1967): Spravochnik po Klimatu SSSR. Kirgizskaya SSR. (in Russian). Leningrad.

GoKR; Davletkeldiev, A. and Takenov, Z. (eds.) (2009): The Kyrgyz Republic's second national communication to the United Nations Framework Convention. Bishkek.

Gurgel, H. C. and Ferreira, N. J. (2003): Annual and interannual variability of NDVI in Brazil and its

connections with climate. In: International Journal of Remote Sensing 24, 3595–3609. https://doi.org/10.1080/0143116021000053788

Hijioka, Y.; Lin, E.; Pereira, J.J.; Corlett, R.T.; Cui, X.; Insarov, G.E.; Lasco, R.D.; Lindgren, E. and Surjan, A. (2014): Asia. Climate Change 2014: impacts, adaptation, and vulnerability. Part B: Regional aspects. Contribution of Working Group II to the Fifth Assessment Report of the Intergovernmental Panel on Climate Change. 1327–1370.

Hu, Z.; Zhang, C.; Hu, Q.; Tian, H.; Hu, Z.; Zhang, C.; Hu, Q. and Tian, H. (2014): Temperature changes in Central Asia from 1979 to 2011 based on multiple datasets. In: Journal of Climate 27, 1143–1167. https://doi.org/10.1175/JCLI-D-13-00064.1

Huang, A.; Zhou, Y.; Zhang, Y.; Huang, D.; Zhao, Y.; Wu, H.; Huang, A.; Zhou, Y.; Zhang, Y.; Huang, D.; Zhao, Y. and Wu, H. (2014): Changes of the annual precipitation over Central Asia in the twenty-first century projected by multimodels of CMIP5. In: Journal of Climate 27, 6627–6646. https://doi.org/10.1175/JCLI-D-14-00070.1

Ichii, K.; Kawabata, a. and Yamaguchi, Y. (2002): Global correlation analysis for NDVI and climatic variables and NDVI trends: 1982-1990. In: International Journal of Remote Sensing 23, 3873–3878. https://doi.org/10.1080/01431160110119416

Kariyeva, J. and Van Leeuwen, W. (2011): Environmental drivers of NDVI-based vegetation phenology in Central Asia. In: Remote Sensing 3, 203–246. https://doi.org/10.3390/rs3020203

Kariyeva, J. and van Leeuwen, W. J. D. (2012): Phenological dynamics of irrigated and natural drylands in Central Asia before and after the USSR collapse. In: Agriculture, Ecosystems and Environment 162, 77–89. https://doi.org/10.1016/j.agee.2012.08.006

Kariyeva, J.; Leeuwen, W. J. D. van and Woodhouse, C. A. (2012): Impacts of climate gradients on the vegetation phenology of major land use types in Central Asia (1981-2008). In: Frontiers of Earth Science 6, 206–225. https://doi.org/10.1007/S11707-012-0315-1

Kerven; C.; Steimann; B.; Ashley; L.; Dear; C. and ur Rahim; I. (2011): Pastoralism and farming in Central Asia's mountains: a research review. MSRC Background Paper No. 1. Bishkek

Klein, I.; Gessner, U. and Kuenzer, C. (2012): Regional land cover mapping and change detection in Central Asia using MODIS time-series. In: Applied Geography 35, 219–234. https://doi.org/10.1016/j.apgeog.2012.06.016

Lai, C.; Chen, X.; Wang, Z.; Wu, X.; Zhao, S.; Wu, X. and Bai, W. (2016): Spatio-temporal variation in rainfall erosivity during 1960–2012 in the Pearl River Basin, China. In: CATENA 137, 382–391. https://doi.org/10.1016/j.catena.2015.10.008

Li, Z.; Li, X.; Wei, D.; Xu, X. and Wang, H. (2010): An assessment of correlation on MODIS-NDVI and EVI with natural vegetation coverage in Northern Hebei Province, China. In: Procedia Environmental Sciences 2, 964–969. https://doi.org/10.1016/j.proenv.2010.10.108

Lioubimtseva, E. and Cole, R. (2006): Uncertainties of climate change in arid environments of Central Asia. In: Reviews in Fisheries Science 14, 29–49. https://doi.org/10.1080/10641260500340603

Lioubimtseva, E. and Henebry, G. M. (2009): Climate and environmental change in arid Central Asia: impacts, vulnerability, and adaptations. In: Journal of Arid Environments 73, 963–977. https://doi.org/10.1016/j.jaridenv.2009.04.022

Lioubimtseva, E.; Cole, R.; Adams, J. M. and Kapustin, G. (2005): Impacts of climate and land-cover changes in arid lands of Central Asia. In: Journal of Arid Environments 62, 285–308. https://doi.org/10.1016/j.jaridenv.2004.11.005

Martinez, B. and Gilabert, M. A. (2009): Vegetation dynamics from NDVI time series analysis using the wavelet transform. In: Remote Sensing of Environment 113, 1823–1842. https://doi.org/10.1016/j.rse.2009.04.016

Mennis, J. (2010): Multidimensional map algebra: design and implementation of a spatio-temporal GIS processing language. In: Transactions in GIS 14, 1–21. https://doi.org/10.1111/j.1467-9671.2009.01179.x

Mennis, J.; Viger, R. and Tomlin, C. D. (2005): Cubic map algebra functions for spatio-temporal analysis. In: Cartography and Geographic Information Science 32, 17–32. https://doi.org/10.1559/1523040053270765

Miles, J. (2014): R squared, adjusted R squared. In: Wiley StatsRef: Statistics Reference Online. https://doi.org/10.1002/9781118445112.stat06627

Militino, A.; Ugarte, M. and Pérez-Goya, U. (2017): Stochastic spatio-temporal models for analysing NDVI Distribution of GIMMS NDVI3g images. In: Remote Sensing 9, 76. https://doi.org/10.3390/rs9010076

Mohammat, A.; Wang, X.; Xu, X.; Peng, L.; Yang, Y.; Zhang, X.; Myneni, R. B. and Piao, S. (2013): Drought and spring cooling induced recent decrease in vegetation growth in inner Asia. In: Agricultural and Forest Meteorology 178–179, 21–30. https://doi.org/10.1016/j.agrformet.2012.09.014

Nezlin, N. P.; Kostianoy, A. G. and Li, B. L. (2005): Inter-annual variability and interaction of remote-sensed vegetation index and atmospheric precipitation in the Aral Sea region. In: Journal of Arid Environments 62, 677–700. https://doi.org/10.1016/j.jaridenv.2005.01.015

Petitjean, F.; Kurtz, C.; Passat, N. and Gançarski, P. (2012): Spatio-temporal reasoning for the classification of satellite image time series. In: Pattern Recognition Letters 33, 1805–1815. https://doi.org/10.1016/j.patrec.2012.06.009

Potter, C. S. and Brooks, V. (1998): Global analysis of empirical relations between annual climate and seasonality of NDVI. In: International Journal of Remote Sensing 19, 2921–2948. https://doi.org/10.1080/014311698214352

Propastin, P. A.; Kappas, M. and Muratova, N. R. (2008a): A remote sensing based monitoring system for discrimination between climate and human-induced vegetation change in Central Asia. In: Management of Environmental Quality: An International Journal 19, 579–596. https://doi.org/http://dx.doi.org/10.1108/14777830810894256

Propastin, P. A.; Kappas, M. and Muratova, N. R. (2008b): Inter-annual changes in vegetation activities and their relationship to temperature and precipitation in Central Asia from 1982 to 2003. In: Journal of Environmental Informatics 12, 75–87. https://doi.org/10.3808/jei.200800126

Propastin, P. A.; Kappas, M.; Erasmi, S. and Muratova, N. R. (2007): Remote sensing based study on intra-annual dynamics of vegetation and climate in drylands of Kazakhstan. In: Basic and Applied Dryland Research 1, 138–154. https://doi.org/10.1127/badr/1/2007/138

Python Software Foundation (2016): Python language reference, version 3.5.

QGIS Development Team (2017): QGIS geographic information system. Open Source Geospatial Foundation Project. http://www.qgis.org

Qiu, B.; Li, W.; Zhong, M.; Tang, Z. and Chen, C. (2014): Spatiotemporal analysis of vegetation variability and its relationship with climate change in China. In: Geo-spatial Information Science 17, 170–180. https://doi.org/10.1080/10095020.2014.959095

Qiu, B.; Wang, Z.; Tang, Z.; Liu, Z.; Lu, D.; Chen, C. and Chen, N. (2016): A multi-scale spatiotemporal modeling approach to explore vegetation dynamics patterns under global climate change. In: GIScience & Remote Sensing 53, 596–613. https://doi.org/10.1080/15481603.2016.1184741

R Core Team (2016): R: a language and environment for statistical computing. https://www.r-project.org/

Rubin, J. (1967): Optimal classification into groups: an approach for solving the taxonomy problem. In: Journal of Theoretical Biology 15, 103–144. https://doi.org/10.1016/0022-5193(67)90046-X

Schneider, U.; Becker, A.; Finger, P.; Meyer-Christoffer, A.; Rudolf, B. and Ziese, M. (2015): GPCC full data reanalysis version 7.0 at 0.5°: monthly land-surface precipitation from rain-gauges built on GTS-based and historic data. ftp://ftp.dwd.de/pub/data/gpcc/html/fulldata_v7_doi_download.html,. https://doi.org/10.5676/DWD_GPCC/FD_M_V7_050

Schultz, P. A. and Halpert, M. S. (2007): Global analysis of the relationships among a vegetation index, precipitation and land surface temperature. In: International Journal of Remote Sensing. https://doi.org/10.1080/01431169508954590

Small, C. (2012): Spatiotemporal dimensionality and time-space characterization of multitemporal imagery. In: Remote Sensing of Environment 124, 793–809. https://doi.org/10.1016/j.rse.2012.05.031

Song, X.-D.; Brus, D. J.; Liu, F.; Li, D.-C.; Zhao, Y.-G.; Yang, J.-L. and Zhang, G.-L. (2016): Mapping soil organic carbon content by geographically weighted regression: a case study in the Heihe River Basin, China. In: Geoderma 261, 11–22. https://doi.org/10.1016/j.geoderma.2015.06.024

Verbesselt, J.; Hyndman, R.; Zeileis, A. and Culvenor, D. (2010): Phenological change detection while accounting for abrupt and gradual trends in satellite image time series. In: Remote Sensing of Environment 114, 2970–2980. https://doi.org/10.1016/j.rse.2010.08.003

Yin, G.; Hu, Z.; Chen, X. and Tiyip, T. (2016): Vegetation dynamics and its response to climate change in Central Asia. In: Journal of Arid Land 8, 375–388. https://doi.org/10.1007/s40333-016-0043-6

Zhang, C.; Lu, D.; Chen, X.; Zhang, Y.; Maisupova, B. and Tao, Y. (2016a): The spatiotemporal patterns of vegetation coverage and biomass of the temperate deserts in Central Asia and their relationships with climate controls. In: Remote Sensing of Environment 175, 271–281. https://doi.org/10.1016/j.rse.2016.01.002

Zhang, Y.; Gao, J.; Liu, L.; Wang, Z.; Ding, M. and Yang, X. (2013): NDVI-based vegetation changes and their responses to climate change from 1982 to 2011: a case study in the Koshi River Basin in the middle Himalayas. In: Global and Planetary Change 108, 139–148. https://doi.org/10.1016/j.gloplacha.2013.06.012

Zhang, Y.; Zhang, C.; Wang, Z.; Chen, Y.; Gang, C.; An, R. and Li, J. (2016b): Vegetation dynamics and its driving forces from climate change and human activities in the Three-River Source Region, China from 1982 to 2012. In: Science of the Total Environment 563, 210–220. https://doi.org/10.1016/j.scitotenv.2016.03.223

Zhao, X.; Tan, K.; Zhao, S. and Fang, J. (2011): Changing climate affects vegetation growth in the arid region of the northwestern China. In: Journal of Arid Environments 75, 946–952. https://doi.org/10.1016/j.jaridenv.2011.05.007

Zhou, J.; Cai, W.; Qin, Y.; Lai, L.; Guan, T.; Zhang, X.; Jiang, L.; Du, H.; Yang, D.; Cong, Z. and Zheng, Y. (2016):

Alpine vegetation phenology dynamic over 16years and its covariation with climate in a semi-arid region of China. In: Science of the Total Environment 572, 119–128. https://doi.org/10.1016/j.scitotenv.2016.07.206

Zhou, Y.; Zhang, L.; Fensholt, R.; Wang, K.; Vitkovskaya, I. and Tian, F. (2015): Climate contributions to vegetation variations in Central Asian drylands: pre- and post-USSR collapse. In: Remote Sensing 7, 2449–2470. https://doi.org/10.3390/rs70302449

Authors

Maksim Kulikov
CEN Center for Earth System
Research and Sustainability
Institute of Geography
University of Hamburg
Bundesstraße 55
20146 Hamburg
Germany
maksim.s.kulikov@gmail.com

Prof. Dr. Udo Schickhoff
CEN Center for Earth System
Research and Sustainability
Institute of Geography
University of Hamburg
Bundesstraße 55
20146 Hamburg
Germany
udo.schickhoff@uni-hamburg.de